NSF Engineering Research Center for Computer Integrated Surgical Systems and Technology

LABORATORY FOR Computational Sensing + Robotics THE JOHNS HOPKINS UNIVERSITY

Registration – Part 2

600.455/655 Computer Integrated Surgery

Russell H. Taylor
John C. Malone Professor of Computer Science,
with joint appointments in Mechanical Engineering, Radiology & Surgery
Director, Laboratory for Computational Sensing and Robotics
The Johns Hopkins University
rht@jhu.edu

100 YEARS JOHNS HOPKINS ENGINEERING

WHITING SCHOOL OF ENGINEERING
THE JOHNS HOPKINS UNIVERSITY

1

Feature-Based 2D-3D Registration

Given

– 3D surface model of an anatomic structure
– Multiple 2D x-ray projection images taken at known poses relative to some coordinate system C
– Initial estimate of the pose **F** of the anatomic object relative to the x-ray imaging coordinate system C

Goal

– Compute an accurate value for **F**

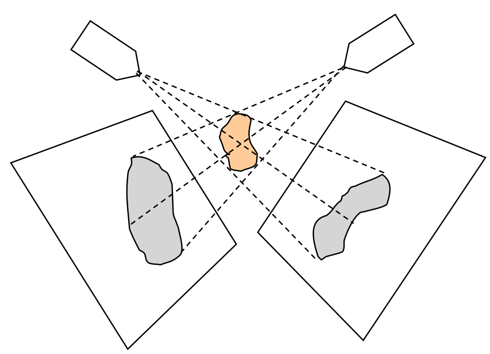

Copyright 2023 R. H. Taylor

2

Feature-Based 2D-3D Registration

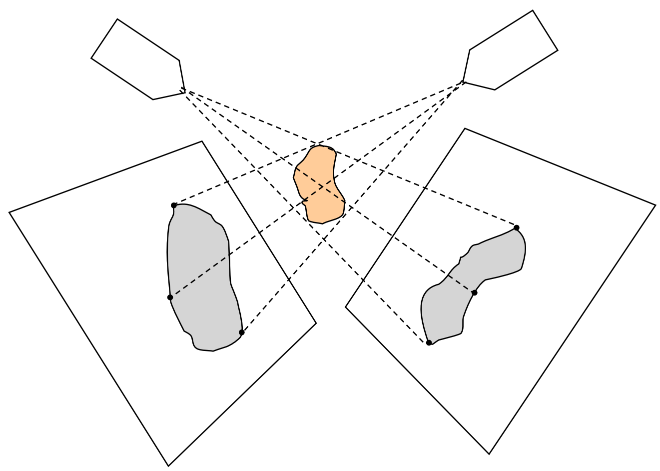

Copyright 2023 R. H. Taylor

3

Feature-Based 2D-3D Registration

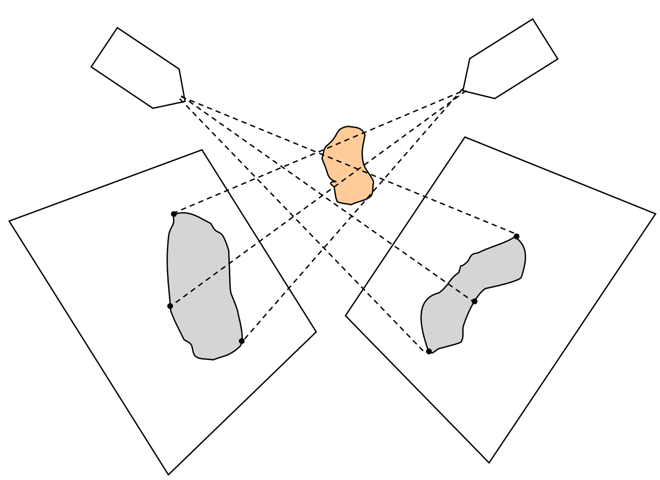

Copyright 2023 R. H. Taylor

4

Feature-Based 2D-3D Registration

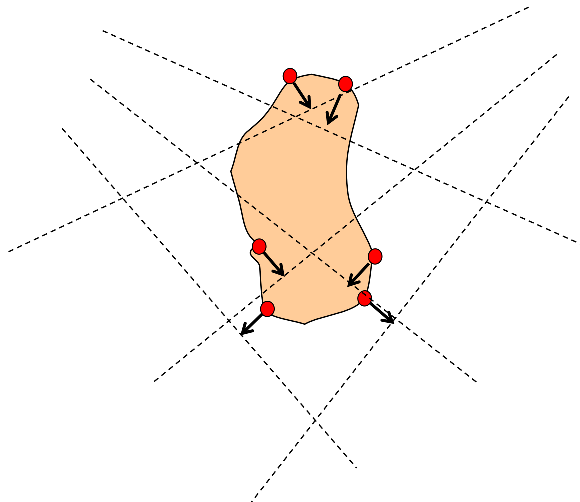

Copyright 2023 R. H. Taylor

Engineering Research Center for Computer Integrated Surgical Systems and Technology

5

Feature-Based 2D-3D Registration

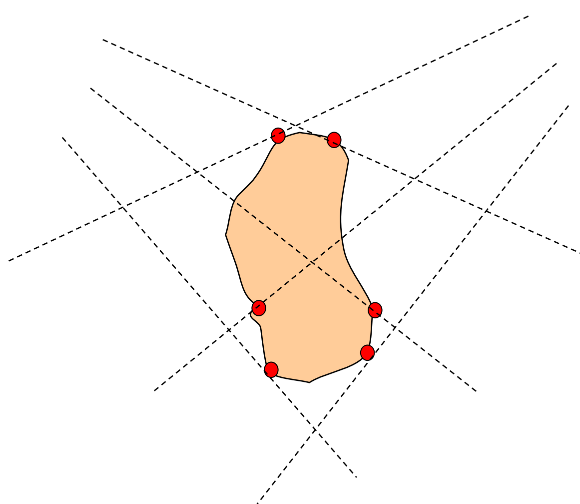

Copyright 2023 R. H. Taylor

Engineering Research Center for Computer Integrated Surgical Systems and Technology

6

Feature-Based 2D-3D Registration

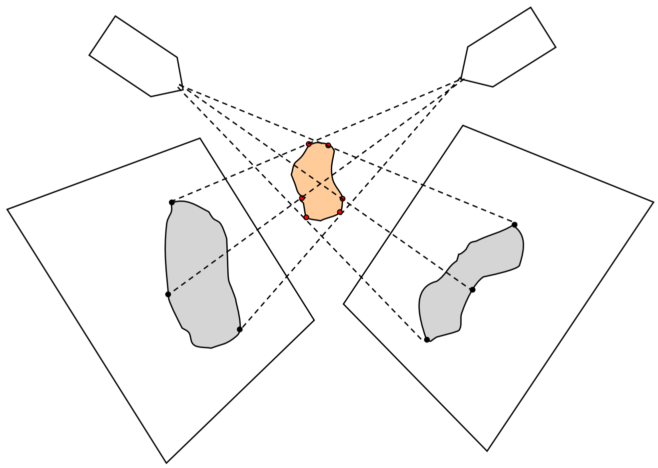

Copyright 2023 R. H. Taylor

7

A contour-based 2D-3D method …

Gueziec *et al., 1998*

Step 0: Extract contours from x-ray images and compute corresponding lines between source and detector

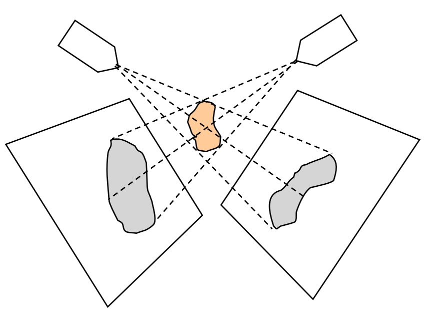

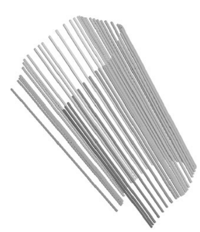

A. Guéziec, P. Kazanzides, B. Williamson, and R. Taylor, "Anatomy-Based Registration of CT-Scan and Intraoperative X-Ray Images for Guiding a Surgical Robot," IEEE Transactions on Medical Imaging, vol. 17, pp. 715-728, 1998.

Copyright 2023 R. H. Taylor

8

A contour-based 2D-3D method …

Gueziec *et al., 1998*

Step 1: Given the current estimate for F = [R,t] ,
compute the apparent projection contours of the model for each viewing direction.

Step 2: For each x-ray path line line L_i, identify the closest point p_i on an apparent projection contour. This will give a set of points on the body surface to be moved toward the corresponding x-ray lines

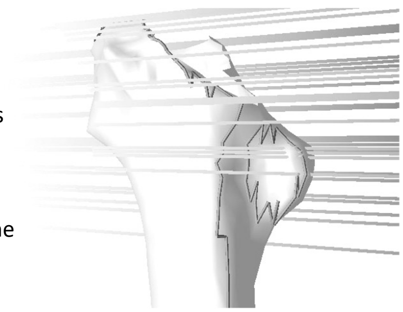

A. Guéziec, P. Kazanzides, B. Williamson, and R. Taylor, "Anatomy-Based Registration of CT-Scan and Intraoperative X-Ray Images for Guiding a Surgical Robot," IEEE Transactions on Medical Imaging, vol. 17, pp. 715-728, 1998.

Copyright 2023 R. H. Taylor

9

A contour-based 2D-3D method …

Gueziec *et al., 1998*

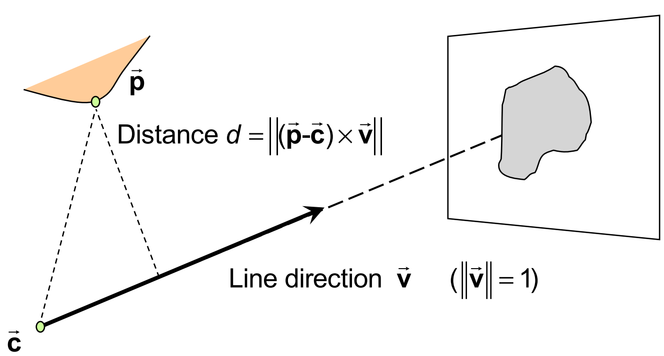

Note: It is convenient to use the x-ray source position (i.e., the center of convergence for a bundle of x-ray projection lines) as the value for $\vec{\mathbf{c}}$.

A. Guéziec, P. Kazanzides, B. Williamson, and R. Taylor, "Anatomy-Based Registration of CT-Scan and Intraoperative X-Ray Images for Guiding a Surgical Robot," IEEE Transactions on Medical Imaging, vol. 17, pp. 715-728, 1998.

Copyright 2023 R. H. Taylor

10

A contour-based 2D-3D method ...

Gueziec *et al., 1998*

Step 3: Solve an optimization problem to compute a value of F that minimizes the distance between the p_i and the L_i.

$$\min_{\mathbf{R},\vec{\mathbf{t}}} \sum_i d_i^2 = \min_{\mathbf{R},\vec{\mathbf{t}}} \sum_i \left\| \vec{\mathbf{v}}_i \times \left(\mathbf{c}_i - \left(\mathbf{R}\vec{\mathbf{p}}_i + \vec{\mathbf{t}} \right) \right) \right\|^2$$

$$= \min_{\mathbf{R},\vec{\mathbf{t}}} \sum_i \left\| skew\left(\vec{\mathbf{v}}_i \right) \bullet \left(\mathbf{c}_i - \left(\mathbf{R}\vec{\mathbf{p}}_i + \vec{\mathbf{t}} \right) \right) \right\|^2$$

Step 4: Iterate steps 1-3 until reach convergence

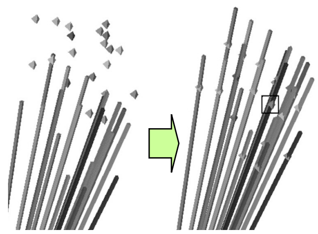

A. Guéziec, P. Kazanzides, B. Williamson, and R. Taylor, "Anatomy-Based Registration of CT-Scan and Intraoperative X-Ray Images for Guiding a Surgical Robot," IEEE Transactions on Medical Imaging, vol. 17, pp. 715-728, 1998.

Copyright 2023 R. H. Taylor

11

Computational Note

Gueziec uses the Cayley parameterization for rotations:

$$\mathbf{R}(\vec{\mathbf{u}}) = \left(\mathbf{I}\text{-skew}(\vec{\mathbf{u}})\right)\left(\mathbf{I}\text{+skew}(\vec{\mathbf{u}})\right)^{-1}$$

This leads to the approximation

$$\mathbf{R}(\vec{\mathbf{u}}) \approx \mathbf{I}\text{+skew}(2\vec{\mathbf{u}})$$

which is similar to our familiar $\mathbf{R}(\vec{\alpha}) \approx \mathbf{I}\text{+skew}(\vec{\alpha})$.

He also uses the notation $\mathbf{U}\text{=skew}(\vec{\mathbf{u}})$. So $\mathbf{R}(\vec{\mathbf{u}}) = (\mathbf{I}-\mathbf{U})(\mathbf{I}+\mathbf{U})^{-1}$

Similarly, we will see $\mathbf{V}\text{=skew}(\vec{\mathbf{v}})$, etc.

Copyright 2023 R. H. Taylor

12

A countour-based 2D-3D method …
Gueziec et al., 1998

Gueziec compared three different methods for performing the minimization in Step 3:

- Levenberg Marquardt (LM) nonlinear minimization.
- Linearization and constrained minimization
- Use of a Robust M-Estimator

A. Guéziec, P. Kazanzides, B. Williamson, and R. Taylor, "Anatomy-Based Registration of CT-Scan and Intraoperative X-Ray Images for Guiding a Surgical Robot," IEEE Transactions on Medical Imaging, vol. 17, pp. 715-728, 1998.

Copyright 2023 R. H. Taylor

13

Levenberg-Marquardt …
(Following development in Gueziec et al., 1998)

Define $f_i(\vec{x}) = \left\| \mathbf{V}_i \left(\vec{\mathbf{c}}_i - \mathbf{R}(\vec{\mathbf{u}})\vec{\mathbf{p}}_i - \vec{\mathbf{t}} \right) \right\|$ where $\vec{x}^t = [\vec{\mathbf{u}}^t, \vec{\mathbf{t}}^t], \mathbf{V}_i = skew(\vec{\mathbf{v}}_i)$

Our goal is to minimize

$$\varepsilon(\vec{x}) = \sum_i f_i(\vec{x})^2 = \sum_i \left\| \mathbf{V}_i \left(\vec{\mathbf{c}}_i - \mathbf{R}(\vec{\mathbf{u}})\vec{\mathbf{p}}_i - \vec{\mathbf{t}} \right) \right\|^2$$

We note that $\varepsilon(\vec{x})$ is nonlinear. Levenberg-Marquardt is a widely used optimization method for problems of this type. However, it requires us to evaluate the partial derivitives $\partial f_i / \partial x_j$. Gueziec worked these out symbolically for his problem

A. Guéziec, P. Kazanzides, B. Williamson, and R. Taylor, "Anatomy-Based Registration of CT-Scan and Intraoperative X-Ray Images for Guiding a Surgical Robot," IEEE Transactions on Medical Imaging, vol. 17, pp. 715-728, 1998.

Copyright 2023 R. H. Taylor

Engineering Research Center for Computer Integrated Surgical Systems and Technology

14

Levenberg-Marquardt ...

(Following development in Gueziec et al., 1998)

Define $f_i(\vec{x}) = \left\| \mathbf{V}_i \left(\vec{\mathbf{c}}_i - \mathbf{R}(\vec{\mathbf{u}})\vec{\mathbf{p}}_i - \vec{\mathbf{t}} \right) \right\|$ where $\vec{x}^t = [\vec{\mathbf{u}}^t, \vec{\mathbf{t}}^t], \mathbf{V}_i = skew(\vec{\mathbf{v}}_i)$

$$\mathbf{J} = \begin{bmatrix} \cdots & \frac{\partial f_i}{\partial \vec{x}} & \cdots \end{bmatrix} = \begin{bmatrix} \cdots & \begin{matrix} \frac{\partial f_i}{\partial \vec{\mathbf{u}}} \\ \frac{\partial f_i}{\partial \vec{\mathbf{t}}} \end{matrix} & \cdots \end{bmatrix}$$

$$\frac{\partial f_i}{\partial \vec{\mathbf{t}}} = \frac{\mathbf{V}_i^t \mathbf{V}_i (\mathbf{R}\vec{\mathbf{p}}_i - \mathbf{c} + \vec{\mathbf{t}})}{f_i}$$

$$\frac{\partial f_i}{\partial \vec{\mathbf{u}}} = \left(\frac{\partial \mathbf{R}\vec{\mathbf{p}}_i}{\partial \vec{\mathbf{u}}} \right)^t \frac{\mathbf{V}_i^t \mathbf{V}_i (\mathbf{R}\vec{\mathbf{p}}_i - \mathbf{c} + \vec{\mathbf{t}})}{f_i}$$

Details on this may be found in reference [45] of Gueziec's paper

A. Guéziec, P. Kazanzides, B. Williamson, and R. Taylor, "Anatomy-Based Registration of CT-Scan and Intraoperative X-Ray Images for Guiding a Surgical Robot," IEEE Transactions on Medical Imaging, vol. 17, pp. 715-728, 1998.

Copyright 2023 R. H. Taylor

Levenberg-Marquardt ...

(Following development in Gueziec et al., 1998)

Step 1: Pick λ = a small number; pick initial guess for $\vec{x}$

Step 2: Evaluate $f_i(\vec{x})$ and $\mathbf{J}$ and solve the least squares problem

$$\begin{bmatrix} \vdots \\ (\mathbf{J}^t\mathbf{J} + \lambda\mathbf{I})\Delta\vec{x} - \mathbf{J}^t f_i \\ \vdots \end{bmatrix} = \begin{bmatrix} \vdots \\ 0 \\ \vdots \end{bmatrix}$$

for $\Delta\vec{x}$.

Step 3: $\vec{x} \leftarrow \vec{x} + \Delta\vec{x}$; update λ.

Step 4: Evaluate termination condition. If not done, go back to to step 2

Note: Usually λ starts small and grows larger. Consult standard references (e.g., Numerical Recipes) for more information.

A. Guéziec, P. Kazanzides, B. Williamson, and R. Taylor, "Anatomy-Based Registration of CT-Scan and Intraoperative X-Ray Images for Guiding a Surgical Robot," IEEE Transactions on Medical Imaging, vol. 17, pp. 715-728, 1998.

Copyright 2023 R. H. Taylor

Constrained Linearized Least Squares …

(Following development in Gueziec et al., 1998)

Step 0: Make an initial guess for $\mathbf{R}$ and $\vec{\mathbf{t}}$

Step 1: Compute $\vec{\mathbf{p}}_i \leftarrow \mathbf{R}\vec{\mathbf{p}}_i + \vec{\mathbf{t}}$

Step 2: Define $\mathbf{P}_i = skew(\vec{\mathbf{p}}_i)$, $\mathbf{V}_i = skew(\vec{\mathbf{v}}_i)$

Step 3: Solve the least squares problem:

$$\varepsilon^2 = \min \left\| \begin{bmatrix} \vdots & \vdots \\ 2\mathbf{V}_i\mathbf{P}_i & \mathbf{V}_i \\ \vdots & \vdots \end{bmatrix} \begin{bmatrix} \vec{\mathbf{u}} \\ \Delta\vec{\mathbf{t}} \end{bmatrix} - \begin{bmatrix} \vdots \\ \mathbf{V}_i(\vec{\mathbf{c}}_i - \vec{\mathbf{p}}_i) \\ \vdots \end{bmatrix} \right\|^2 \quad \text{subject to } \|\vec{\mathbf{u}}\| \le \rho$$

where ρ is sufficiently small so that $\mathbf{I}+2\mathbf{U}$ approximates a rotation

Step 4: Compute $\Delta\mathbf{R} = (\mathbf{I} - \mathbf{U})(\mathbf{I} + \mathbf{U})^{-1}$

Update $\mathbf{p}_i \leftarrow \Delta\mathbf{R}\mathbf{p}_i + \Delta\vec{\mathbf{t}}$; $\mathbf{R} \leftarrow \Delta\mathbf{R}\mathbf{R}$; $\vec{\mathbf{t}} \leftarrow \Delta\mathbf{R}\vec{\mathbf{t}} + \Delta\vec{\mathbf{t}}$

Step 5: If ε is small enough or some othe termination condition is met, then stop. Otherwise go back to Step 2.

A. Guéziec, P. Kazanzides, B. Williamson, and R. Taylor, "Anatomy-Based Registration of CT-Scan and Intraoperative X-Ray Images for Guiding a Surgical Robot," IEEE Transactions on Medical Imaging, vol. 17, pp. 715-728, 1998.

Copyright 2023 R. H. Taylor

Robust Pose Estimation …

- Basic idea is to identify outliers and give them little or no weight.

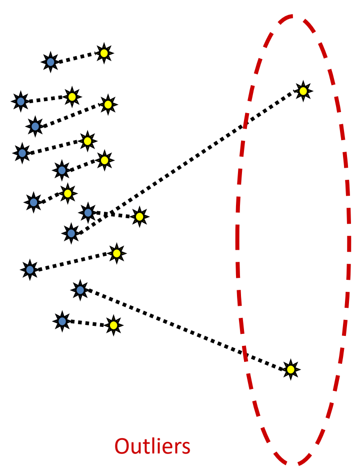

R. Kumar and A. R. Hanson, "Robust methods for estimating pose and a sensitivity analysis," Comput. Vision, Graphics, Image Processing-IU, vol. 60, no. 3, pp. 313–342, 1994.

Copyright 2023 R. H. Taylor

Robust Pose Estimation …

- Basic idea is to identify outliers and give them little or no weight.

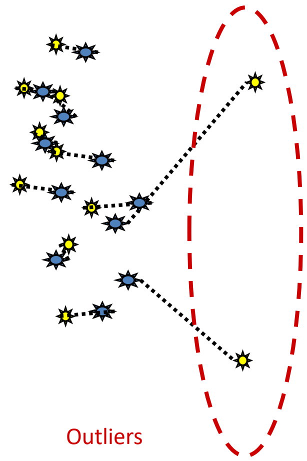

R. Kumar and A. R. Hanson, "Robust methods for estimating pose and a sensitivity analysis," Comput. Vision, Graphics, Image Processing-IU, vol. 60, no. 3, pp. 313–342, 1994.

Copyright 2023 R. H. Taylor

19

Robust Pose Estimation …

- Basic idea is to identify outliers and give them little or no weight.

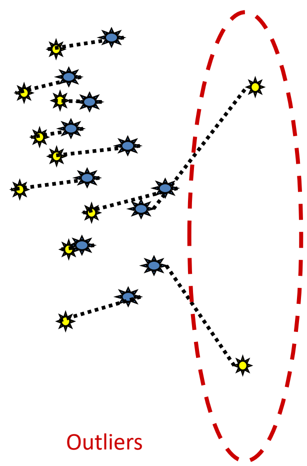

R. Kumar and A. R. Hanson, "Robust methods for estimating pose and a sensitivity analysis," Comput. Vision, Graphics, Image Processing-IU, vol. 60, no. 3, pp. 313–342, 1994.

Copyright 2023 R. H. Taylor

20

Robust Pose Estimation …

- Basic idea is to identify outliers and give them little or no weight.

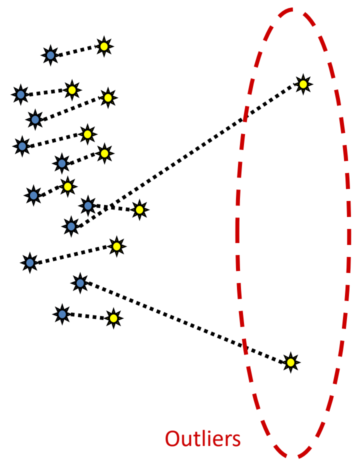

R. Kumar and A. R. Hanson, "Robust methods for estimating pose and a sensitivity analysis," Comput. Vision, Graphics, Image Processing-IU, vol. 60, no. 3, pp. 313–342, 1994.

Copyright 2023 R. H. Taylor

Robust Pose Estimation …

- Basic idea is to identify outliers and give them little or no weight.

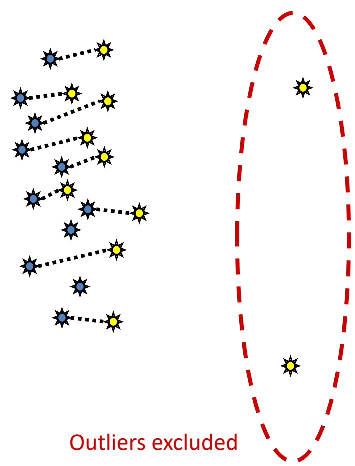

R. Kumar and A. R. Hanson, "Robust methods for estimating pose and a sensitivity analysis," Comput. Vision, Graphics, Image Processing-IU, vol. 60, no. 3, pp. 313–342, 1994.

Copyright 2023 R. H. Taylor

Robust Pose Estimation …

- Basic idea is to identify outliers and give them little or no weight.

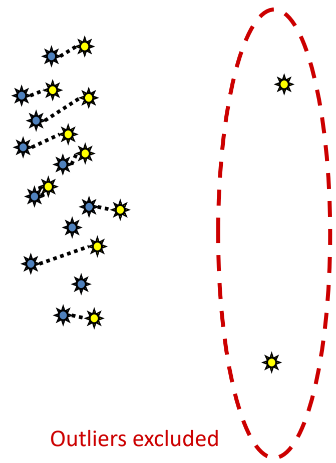

R. Kumar and A. R. Hanson, “Robust methods for estimating pose and a sensitivity analysis,” Comput. Vision, Graphics, Image Processing-IU, vol. 60, no. 3, pp. 313–342, 1994.

Copyright 2023 R. H. Taylor

23

Robust Pose Estimation …

- Basic idea is to identify outliers and give them little or no weight.

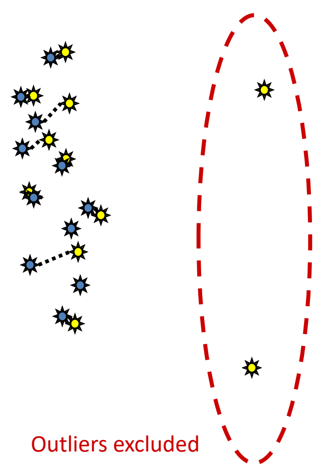

R. Kumar and A. R. Hanson, “Robust methods for estimating pose and a sensitivity analysis,” Comput. Vision, Graphics, Image Processing-IU, vol. 60, no. 3, pp. 313–342, 1994.

Copyright 2023 R. H. Taylor

24

Robust M-Estimator …

(Following development in Gueziec et al., 1998)

Step 0: Make an initial guess for $\mathbf{R}$ and $\vec{\mathbf{t}}$

Step 1: Compute $\vec{\mathbf{p}}_i \leftarrow \mathbf{R}\vec{\mathbf{p}}_i + \vec{\mathbf{t}}$

Step 2: Define $\mathbf{P}_i = skew(\vec{\mathbf{p}}_i)$, $\mathbf{V}_i = skew(\vec{\mathbf{v}}_i)$,

Step 3: Solve a robust linearized problem

$$\varepsilon = \underset{\vec{\mathbf{u}},\Delta\vec{\mathbf{t}}}{\arg\min} \sum_i \rho\left(\frac{0.6745\ e_i}{median(\{e_i\})}\right) \quad \text{where } e_i = \left\|\mathbf{V}_i(\vec{\mathbf{p}}_i - \mathbf{c}_i + 2\mathbf{P}_i\vec{\mathbf{u}} + \Delta\vec{\mathbf{t}})\right\|$$

(See next slide)

Step 4: Compute $\Delta\mathbf{R} = (\mathbf{I} - \mathbf{U})(\mathbf{I} + \mathbf{U})^{-1}$

Update $\mathbf{p}_i \leftarrow \Delta\mathbf{R}\mathbf{p}_i + \Delta\vec{\mathbf{t}}$; $\mathbf{R} \leftarrow \Delta\mathbf{R}\mathbf{R}$; $\vec{\mathbf{t}} \leftarrow \Delta\mathbf{R}\vec{\mathbf{t}} + \Delta\vec{\mathbf{t}}$

Step 5: If ε is small enough or some othe termination condition is met, then stop. Otherwise go back to Step 2.

A. Guéziec, P. Kazanzides, B. Williamson, and R. Taylor, "Anatomy-Based Registration of CT-Scan and Intraoperative X-Ray Images for Guiding a Surgical Robot," IEEE Transactions on Medical Imaging, vol. 17, pp. 715-728, 1998.

Copyright 2023 R. H. Taylor

25

Robust M-Estimator …

(Following development in Gueziec et al., 1998)

Step 3.0: Set $\vec{\mathbf{u}} = \vec{\mathbf{0}}$, $\Delta\mathbf{t} = \vec{\mathbf{0}}$

Step 3.1: Compute $e_i = \left\|\mathbf{V}_i(\vec{\mathbf{p}}_i - \vec{\mathbf{c}}_i + 2P_i\vec{\mathbf{u}} + \Delta\vec{\mathbf{t}})\right\|$, $s = median(\{\cdots, e_i, \cdots\}) / 0.6745$,

Step 3.2: Solve $\mathbf{C}\vec{x} = \vec{\mathbf{d}}$, where $\vec{x}^t = [\vec{\mathbf{u}}^t, \vec{\mathbf{t}}^t]$

$$\mathbf{C} = \sum_i \Psi\left(\frac{e_i}{s}\right)\begin{bmatrix} 2\mathbf{P}_i\mathbf{W}_i\mathbf{P}_i & \mathbf{P}_i\mathbf{W}_i \\ 2\mathbf{P}_i\mathbf{W}_i & \mathbf{W}_i \end{bmatrix} \text{ and } \vec{\mathbf{d}} = \sum_i \Psi\left(\frac{e_i}{s}\right)\begin{bmatrix} \mathbf{P}_i\mathbf{W}_i(\vec{\mathbf{c}}_i - \vec{\mathbf{p}}_i) \\ \mathbf{W}_i(\vec{\mathbf{c}}_i - \vec{\mathbf{p}}_i) \end{bmatrix}$$

$$\text{where } \mathbf{W}_i = \mathbf{V}_i^t\mathbf{V}_i = \mathbf{I} - \vec{\mathbf{v}}_i\mathbf{v}_i^t \quad \Psi(\mu) = \begin{cases} \mu\left(1 - \mu^2/\alpha^2\right)^2 & \text{if } \|\mu\| \le \alpha \\ 0 & \text{otherwise} \end{cases}$$

(**Note**: We use α=2)

Step 3.3: Iterate steps 3.1 and 3.2 until a suitable termination condition is reached.

A. Guéziec, P. Kazanzides, B. Williamson, and R. Taylor, "Anatomy-Based Registration of CT-Scan and Intraoperative X-Ray Images for Guiding a Surgical Robot," IEEE Transactions on Medical Imaging, vol. 17, pp. 715-728, 1998.

Copyright 2023 R. H. Taylor

26

A countour-based 2D-3D method … results

Gueziec *et al., 1998*

Before

After

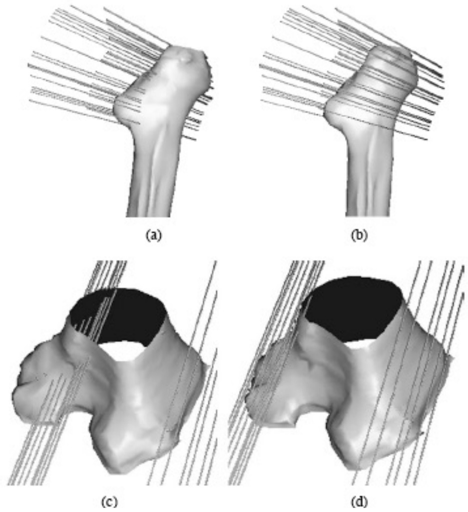

A. Guéziec, P. Kazanzides, B. Williamson, and R. Taylor, "Anatomy-Based Registration of CT-Scan and Intraoperative X-Ray Images for Guiding a Surgical Robot," IEEE Transactions on Medical Imaging, vol. 17, pp. 715-728, 1998.

Copyright 2023 R. H. Taylor

Engineering Research Center for Computer Integrated Surgical Systems and Technology

27

A countour-based 2D-3D method … results

Gueziec *et al., 1998*

Linear

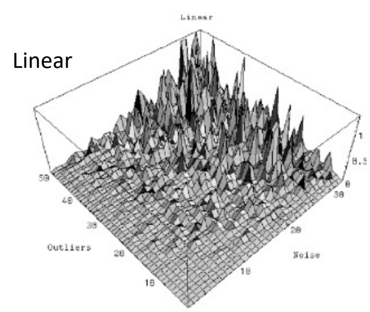

LM

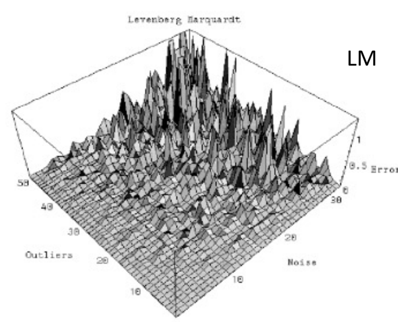

Robust

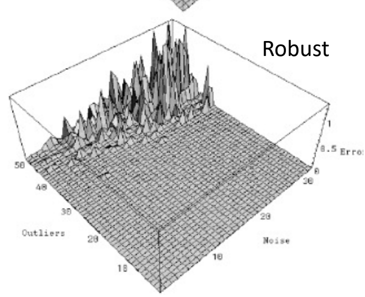

Error *vs* noise and outliers

A. Guéziec, P. Kazanzides, B. Williamson, and R. Taylor, "Anatomy-Based Registration of CT-Scan and Intraoperative X-Ray Images for Guiding a Surgical Robot," IEEE Transactions on Medical Imaging, vol. 17, pp. 715-728, 1998.

Copyright 2023 R. H. Taylor

Engineering Research Center for Computer Integrated Surgical Systems and Technology

28

A contour-based 2D-3D method … times

Gueziec *et al., 1998*

TABLE I
AVERAGE EXECUTION TIMES IN MS FOR THE THREE REGISTRATION METHODS APPLIED TO DATA SETS THAT COMPRISE 100 POINTS (TOP) AND 20 POINTS (BOTTOM)

Number Points/Method	LM	Linear	Robust
100 points (CPU time)	790	690	28
20 points (CPU time)	200	42	9.6

A. Guéziec, P. Kazanzides, B. Williamson, and R. Taylor, "Anatomy-Based Registration of CT-Scan and Intraoperative X-Ray Images for Guiding a Surgical Robot," IEEE Transactions on Medical Imaging, vol. 17, pp. 715-728, 1998.

Copyright 2023 R. H. Taylor

Probabilistic Registration

- Registration methods typically use some optimization algorithm to find a “best” transformation between one data set and the other.
- It makes sense to try to find the “most likely” registration transformation.
- ICP minimizes sum-of-squares distances.
- This is equivalent to assuming that point-pair match probabilities are independent and symmetric Gaussian distributions based on distances
- But there are a number of other methods that explicitly consider probabilities …

Copyright 2023 R. H. Taylor

Coherent Point Drift

- A. Myronenko and X. Song, "Point-Set Registration: Coherent Point Drift", *IEEE Trans. on Pattern Analysis and Machine Intelligence,* vol. 32- 12, pp. 2262-2275, 2010.
- Alignment of point clouds
  - Fast method follows "EM" paradigm
  - Tolerates outliers and noise
  - Transformations: Rigid, affine, general deformable

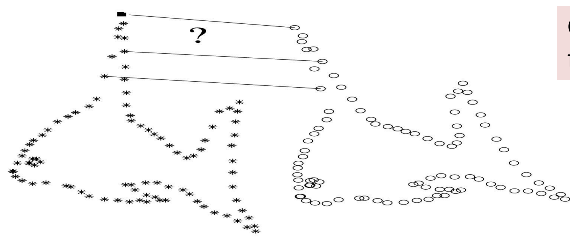

Click here for [slides]

Copyright 2023 R. H. Taylor

44

Registration of intraoperative data to preoperative models

- Want to know registration from tracker to CT space
  - Provides tool positions relative to CT
- Data sources for registration
  - Tracked ultrasound
  - Tracked (or calibrated) range data

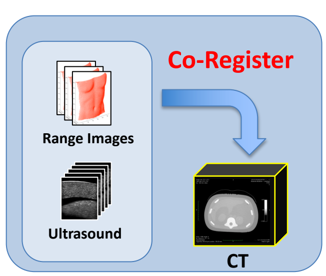

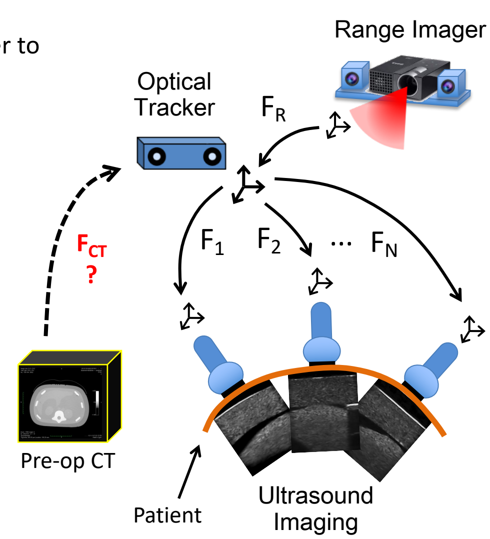

S. Billings and R. H. Taylor, "Iterative Most Likely Oriented Point Registration", *in Medical Image Computing and Computer-Assisted Interventions (MICCAI)*, Boston, October, 2014. (accepted).

Copyright 2023 R. H. Taylor

46

Multi-Modal Feature-Based Registration

Question: How to combine multiple data sources, in order to improve the accuracy and robustness of registration outcomes?

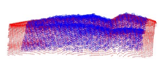

Feature-Based

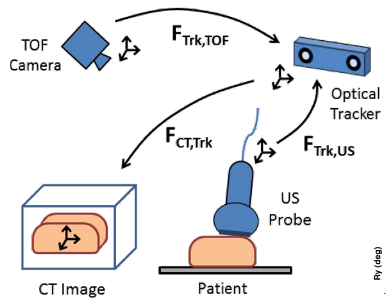

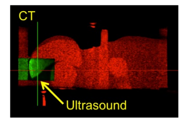

Intensity-Based

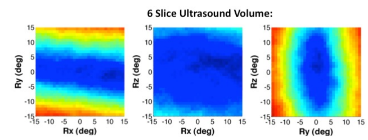

Billings S, Kapoor A, Keil M, Wood BJ, Boctor E (2011) A Hybrid Surface/Image-Based Approach to Facilitate Ultrasound/CT Registration. *SPIE, Medical Imaging 2011: Ultrasonic Imaging, Tomography, and Therapy* 7968: 79680V–79680V-12

47

Example: Clear Guide Medical Navigation System

- Handheld device:
  - low cost
  - integrated on probe
  - ease of use
  - no workflow interruptions
  - in-situ guidance
  - no tool calibration
  - no sterility issues
  - high accuracy
  - real-time fusion
  - real-time quality control

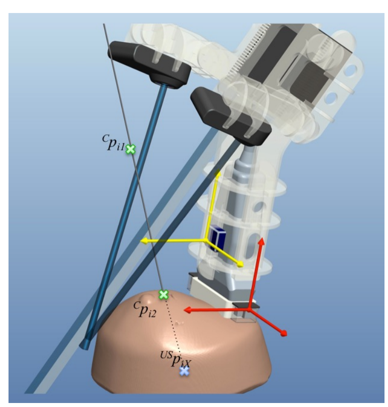

Copyright 2023 R. H. Taylor

Engineering Research Center for Computer Integrated Surgical Systems and Technology

48

Easy-to-Follow Guidance

- CG-1 has traditional ultrasound screen AND on-screen guidance overlay

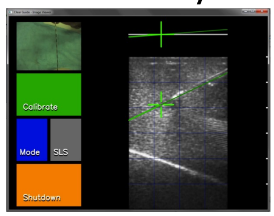

- As well as on-patient projection

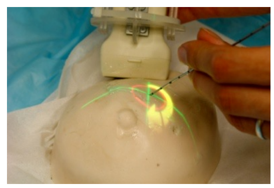

Copyright 2023 R. H. Taylor

Engineering Research Center for Computer Integrated Surgical Systems and Technology

49

Real-time Multi-modal Fusion

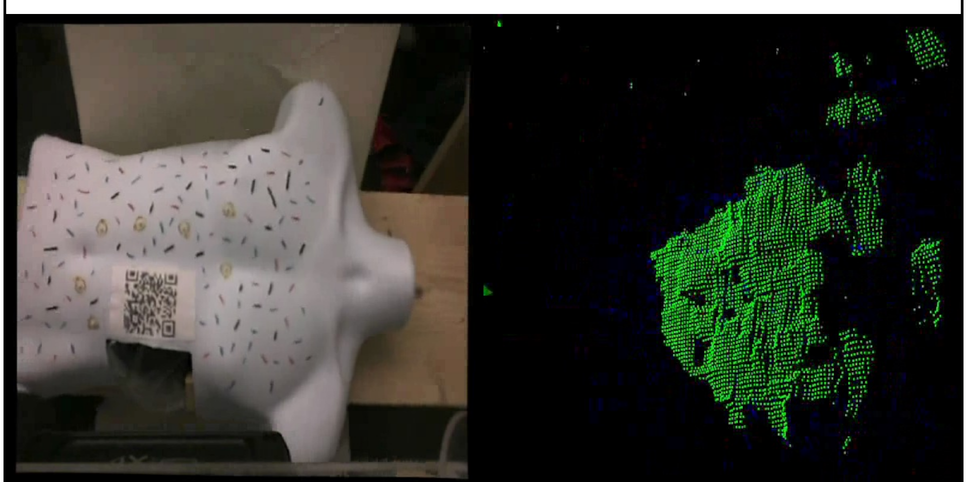

Copyright 2023 R. H. Taylor

Engineering Research Center for Computer Integrated Surgical Systems and Technology

50

Multi-Modal Feature-Based Registration

Question: How to combine multiple data sources, in order to improve the accuracy and robustness of registration outcomes?

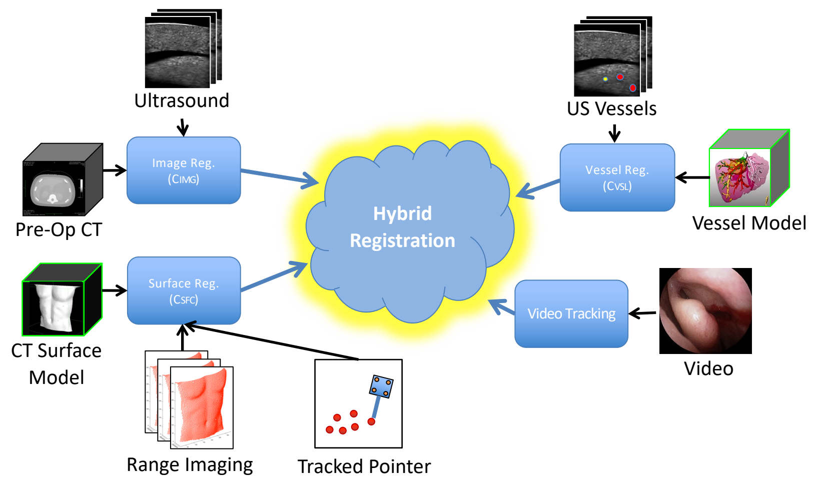

Billings S, Kapoor A, Keil M, Wood BJ, Boctor E (2011) A Hybrid Surface/Image-Based Approach to Facilitate Ultrasound/CT Registration. In: *SPIE, Medical Imaging 2011: Ultrasonic Imaging, Tomography, and Therapy*

51

Multi-Modal Feature-Based Registration

Question: How to combine multiple data sources, in order to improve the accuracy and robustness of registration outcomes?

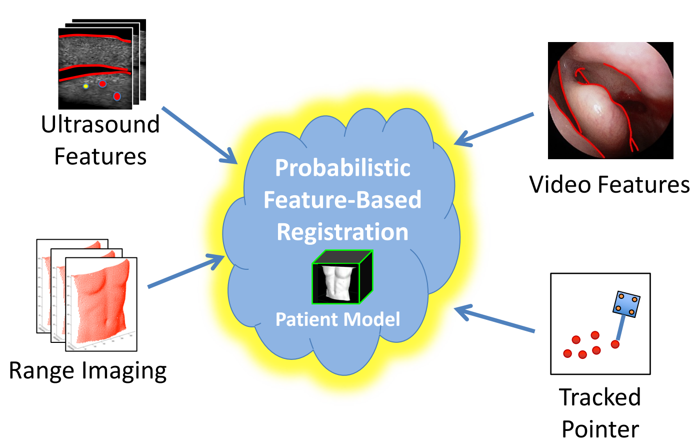

Copyright 2023 R. H. Taylor

Credit: Seth Billings Engineering Research Center for Computer Integrated Surgical Systems and Technology

52

Iterative Closest Point (ICP) Revisited

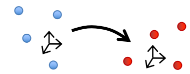

- Widely popular and useful method for point cloud to surface registration introduced by Besl & McKay in 1992
- Many variants proposed since its inception affecting all aspects of the algorithm (robustness, matching criteria, match alignment, etc.)

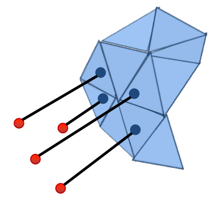

➢ **Matching Phase**:

for each point in the source shape, find the closest point on the target shape

$$\boldsymbol{y_i} = \mathrm{C_{CP}}(T(\boldsymbol{x_i}), \Psi) = \underset{\boldsymbol{y} \in \Psi}{\operatorname{argmin}} \|\boldsymbol{y} - T(\boldsymbol{x_i})\|_2$$

➢ **Registration Phase:**

compute transformation to minimize sum of square distances between matches

$$T = \underset{T}{\operatorname{argmin}} \sum_{i=1}^{n} \|\boldsymbol{y_i} - T(\boldsymbol{x_i})\|_2^2$$

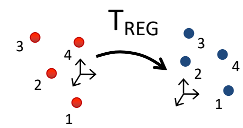

S. Billings and R. H. Taylor, "Iterative Most Likely Oriented Point Registration", *in Medical Image Computing and Computer-Assisted Interventions (MICCAI)*, Boston, October, 2014.

Copyright 2023 R. H. Taylor

Credit: Seth Billings **Engineering Research Center for Computer Integrated Surgical Systems and Technology**

53

Most-Likely Point Paradigm Illustrated with ICP

1. **Probability Model:** isotropic Gaussian

$$f_{\mathrm{match}}(\mathbf{x} \,|\, \mathbf{y}, \sigma^2) = \frac{1}{(2\pi\sigma^2)^{3/2}} \cdot e^{-\frac{1}{2\sigma^2}\|\mathbf{y}-\mathbf{x}\|^2}$$

2. **Match Phase:**

$$\begin{aligned} \mathbf{y}_i &= \underset{\mathbf{y}_i \,\in\, \Psi}{\operatorname{argmax}} \, f_{\mathrm{match}}(\mathrm{T}(\mathbf{x}_i) \,|\, \mathbf{y}_i, \sigma^2) \\ &= \underset{\mathbf{y}_i \,\in\, \Psi}{\operatorname{argmax}} \frac{1}{(2\pi\sigma^2)^{3/2}} \cdot e^{-\frac{1}{2\sigma^2}\|\mathbf{y}_i - \mathrm{T}(\mathbf{x}_i)\|^2} \\ &\rightarrow \underset{\mathbf{y}_i \,\in\, \Psi}{\operatorname{argmin}} \|\mathbf{y}_i - \mathrm{T}(\mathbf{x}_i)\| \end{aligned}$$

3. **Registration Phase:**

$$\begin{aligned} \mathbf{T} &= \underset{\mathbf{T}}{\operatorname{argmax}} \prod_i^n f_{\mathrm{match}}(\mathrm{T}(\mathbf{x}_i) \,|\, \mathbf{y}_i, \sigma^2) \\ &= \underset{\mathbf{T}}{\operatorname{argmax}} \prod_i^n \frac{1}{(2\pi\sigma^2)^{3/2}} \cdot e^{-\frac{1}{2\sigma^2}\|\mathbf{y}_i - \mathrm{T}(\mathbf{x}_i)\|^2} \\ &\rightarrow \underset{\mathbf{T}}{\operatorname{argmax}} \left[-n \log\left((2\pi\sigma^2)^{3/2} \right) - \frac{1}{2\sigma^2} \sum_i^n \|\mathbf{y}_i - \mathrm{T}(\mathbf{x}_i)\|^2 \right] \\ &\rightarrow \underset{\mathbf{T}}{\operatorname{argmin}} \sum_i^n \|\mathbf{y}_i - \mathrm{T}(\mathbf{x}_i)\|^2 \end{aligned}$$

Copyright 2023 R. H. Taylor

Credit: Seth Billings **Engineering Research Center for Computer Integrated Surgical Systems and Technology**

54

Outline of Registration Algorithms

- ICP - Iterative Closest Point
  - isotropic position data
- IMLP - Iterative Most Likely Point
  - anisotropic position data
  - robust to outliers
- IMLOP - Iterative Most Likely Oriented Point
  - isotropic position & orientation data
- G-IMLOP - Generalized IMLOP
  - anisotropic position & orientation data
- P-IMLOP - Projected IMLOP
  - anisotropic position & projected orientation data

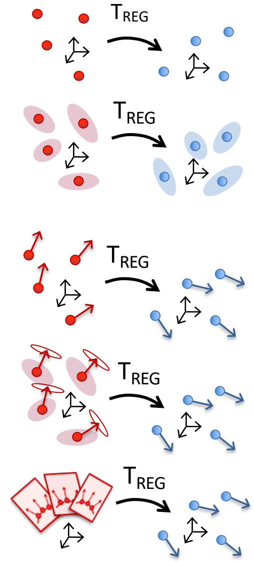

Copyright 2023 R. H. Taylor
Credit: Seth Billings

56

Sources of Anisotropic Uncertainty

Tomographic Imaging

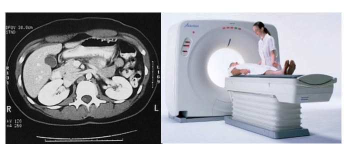

Ultrasound

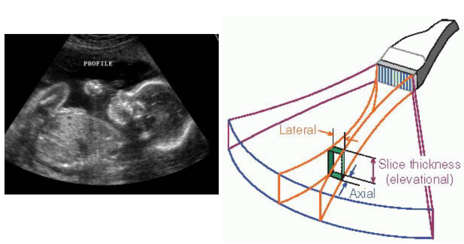

Stereo Vision

Figures: http://www.ndigital.com/wp-content/uploads/2013/09/4col_polarisvicra1.png; *The Essential Physics of Medical Imaging, 3rd ed.*; *http://www.infotech.edu/wp-content/uploads/2013/01/L.A.B.-Look-At-Baby-3D-Ultrasound-Tests-Ultrasound-Technicians-bw-300x225.jpg*; *http://i00.i.aliimg.com/photo/v0/105832128/CT_Scan_equipment.jpg*

Copyright 2023 R. H. Taylor
Credit: Seth Billings

57

Prior Work: Anisotropic Registration

- Generalized Total Least Squares ICP (GTLS-ICP)

  Estépar RSJ, Brun A, Westin C-F (2004) Robust generalized total least squares iterative closest point registration. In: *MICCAI 2004*
  - Registration Phase
    - anisotropic noise model
    - ad-hoc implementation less accurate / efficient; can be unstable
  - Match Phase
    - isotropic (i.e. closest-point matching)

- Generalized ICP (G-ICP)
  - Registration Phase
    - anisotropic noise model limited to model locally-linear surface regions surrounding each feature point of a point cloud shape
    - uses off-the-shelf conjugate gradient solver
  - Match Phase
    - isotropic (i.e. closest-point matching)

Segal A, Haehnel D, Thrun S (2009) Generalized-ICP. In: *Robotics: Science and Systems V*

Copyright 2023 R. H. Taylor
Credit: Seth Billings
Engineering Research Center for Computer Integrated Surgical Systems and Technology

58

Prior Work: Anisotropic Registration

- Anisotropic ICP (A-ICP)

  Maier-Hein L, Franz AM, Dos Santos TR, Schmidt M, Fangerau M, et al. (2012) Convergent iterative closest-point algorithm to accomodate anisotropic and inhomogenous localization error. *IEEE Trans Pattern Anal Mach Intell* 34: 1520–1532.
  - Registration Phase
    - anisotropic noise model
    - ad-hoc implementation does not fully account for noise in both shapes (i.e., lacks ability to reorient the data-shape covariances during optimization)
  - Match Phase
    - anisotropic noise model with non-optimal matching (finds minimal Mahalanobis distance match rather than most-likely match)
    - inefficient implementation; also cannot guarantee that the “best” match is found
  - Initializes registration by ICP (due to inefficient match phase)

Copyright 2023 R. H. Taylor
Credit: Seth Billings
Engineering Research Center for Computer Integrated Surgical Systems and Technology

59

Iterative Most Likely Point (IMLP)

Probability Model: anisotropic Gaussian

$$f_{\text{match}}(\mathbf{x}\,|\,\mathbf{y},\Sigma_{\mathrm{x}},\Sigma_{\mathrm{y}}) = \frac{1}{(2\pi)^{3/2}|\Sigma_{\mathrm{x}}+\Sigma_{\mathrm{y}}|^{1/2}} \cdot e^{-\frac{1}{2}(\mathbf{y}-\mathbf{x})^{T}(\Sigma_{\mathrm{x}}+\Sigma_{\mathrm{y}})^{-1}(\mathbf{y}-\mathbf{x})}$$

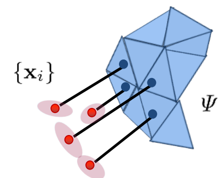

Match Phase:

$$[\mathbf{y}_i,\mathbf{\Sigma}_{\mathrm{y}i}] = \underset{[\mathbf{y}_i,\mathbf{\Sigma}_{\mathrm{y}i}]\,\in\,\Psi}{\operatorname{argmin}} \Big[\log\left|\mathbf{R}\mathbf{\Sigma}_{\mathrm{x}i}\mathbf{R}^{T}+\mathbf{\Sigma}_{\mathrm{y}i}\right| + (\mathbf{y}_i-\mathrm{T}(\mathbf{x}_i))^{T}(\mathbf{R}\mathbf{\Sigma}_{\mathrm{x}i}\mathbf{R}^{T}+\mathbf{\Sigma}_{\mathrm{y}i})^{-1}(\mathbf{y}_i-\mathrm{T}(\mathbf{x}_i)) \Big]$$

Registration Phase:

$$\mathbf{T} = \underset{\mathbf{T}=[\mathbf{R},\mathbf{t}]}{\operatorname{argmin}} \sum_{i}^{n}(\mathbf{y}_i-\mathrm{T}(\mathbf{x}_i))^{T}(\mathbf{R}\mathbf{\Sigma}_{\mathrm{x}i}\mathbf{R}^{T}+\mathbf{\Sigma}_{\mathrm{y}i})^{-1}(\mathbf{y}_i-\mathrm{T}(\mathbf{x}_i))$$

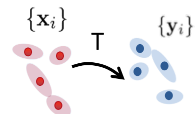

Billings SD, Boctor EM, Taylor RH (2015) Iterative Most-Likely Point Registration (IMLP): A Robust Algorithm for Computing Optimal Shape Alignment. *PLoS One* 10: e0117688

60

IMLP: Match Phase

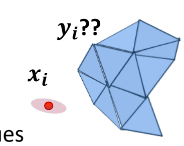

- Due to anisotropic distance metric, standard KD-tree search techniques do not apply.
- **Approach**: PD-tree search with modified node test

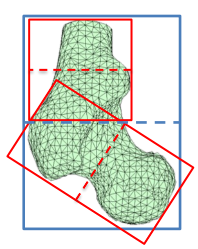

PD Tree Constructed by Datum Positions

Constructing the PD tree:

1. Add all datums to a root node
2. Compute covariance of datum positions within the node
3. Create minimally-sized bounding box aligned to the covariance eigenvectors
4. Partition node along the direction of greatest extent
5. Form left and right child nodes from the datums in each partition
6. Repeat from Step 2 for left and right child nodes until # datums in node < threshold or node size < threshold

Copyright 2023 R. H. Taylor

Credit: Seth Billings

Engineering Research Center for Computer Integrated Surgical Systems and Technology

61

IMLP: Match Phase

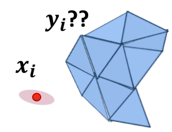

Searching the PD tree:

Assume the current match candidate has a match error equal to E_{best}

Question: can any feature in this node possibly provide a match error less than E_{best}?

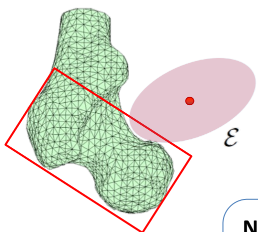

Node of the PD Tree

$$[\mathbf{y}_i, \mathbf{\Sigma}_{yi}] = \underset{[\mathbf{y}_i,\mathbf{\Sigma}_{yi}]\in\Psi}{\operatorname{argmin}} \Big[\log(|\mathbf{R\Sigma}_{xi}\mathbf{R}^T + \mathbf{\Sigma}_{yi}|) + (\mathbf{y}_i - \mathrm{T}(\mathbf{x}_i))^T(\mathbf{R\Sigma}_{xi}\mathbf{R}^T+\mathbf{\Sigma}_{yi})^{-1}(\mathbf{y}_i - \mathrm{T}(\mathbf{x}_i))\Big]$$

True if: $(\mathbf{y}_i - \mathrm{T}(\mathbf{x}_i))^T(\mathbf{R\Sigma}_{xi}\mathbf{R}^T+\mathbf{\Sigma}_{\text{node}})^{-1}(\mathbf{y}_i - \mathrm{T}(\mathbf{x}_i)) < E_{\text{best}} - log_{\min}$

Node Test: if the **ellipsoid**

$$\mathcal{E} = \{\mathbf{y} \mid (\mathbf{y} - \mathrm{T}(\mathbf{x}_i))^T(\mathbf{R\Sigma}_{xi}\mathbf{R}^T+\mathbf{\Sigma}_{\text{node}})^{-1}(\mathbf{y} - \mathrm{T}(\mathbf{x}_i)) \le E_{\text{best}} - log_{\min}\}$$

intersects the bounding box of the node, then search the node

Copyright 2023 R. H. Taylor

Credit: Seth Billings Engineering Research Center for Computer Integrated Surgical Systems and Technology

62

IMLP: Match Phase

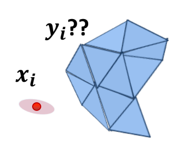

Searching the PD tree:

Assume the current match candidate has a match error equal to E_{best}

Question: can any feature in this node possibly provide a match error less than E_{best}?

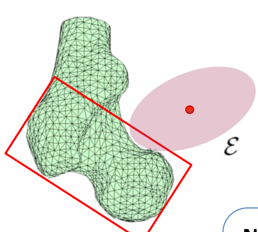

Node of the PD Tree

$$[\mathbf{y}_i, \mathbf{\Sigma}_{yi}] = \underset{[\mathbf{y}_i,\mathbf{\Sigma}_{yi}]\in\Psi}{\operatorname{argmin}} \Big[\log(|\mathbf{R\Sigma}_{xi}\mathbf{R}^T + \mathbf{\Sigma}_{yi}|) + (\mathbf{y}_i - \mathrm{T}(\mathbf{x}_i))^T(\mathbf{R\Sigma}_{xi}\mathbf{R}^T+\mathbf{\Sigma}_{yi})^{-1}(\mathbf{y}_i - \mathrm{T}(\mathbf{x}_i))\Big]$$

True if: $(\mathbf{y}_i - \mathrm{T}(\mathbf{x}_i))^T(\mathbf{R\Sigma}_{xi}\mathbf{R}^T+\mathbf{\Sigma}_{\text{node}})^{-1}(\mathbf{y}_i - \mathrm{T}(\mathbf{x}_i)) < E_{\text{best}} - log_{\min}$

Details in Billings' Thesis

Node Test: if the **ellipsoid**

$$\mathcal{E} = \{\mathbf{y} \mid (\mathbf{y} - \mathrm{T}(\mathbf{x}_i))^T(\mathbf{R\Sigma}_{xi}\mathbf{R}^T+\mathbf{\Sigma}_{\text{node}})^{-1}(\mathbf{y} - \mathrm{T}(\mathbf{x}_i)) \le E_{\text{best}} - log_{\min}\}$$

intersects the bounding box of the node, then search the node

Copyright 2023 R. H. Taylor

Credit: Seth Billings Engineering Research Center for Computer Integrated Surgical Systems and Technology

63

IMLP: Registration Phase

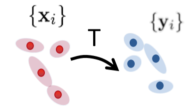

1. Re-formulate the cost function from an unconstrained optimization

$$\mathbf{T} = \underset{[\mathbf{R},\mathbf{t}]}{\operatorname{argmin}} \sum_{i=1}^{n} (\mathbf{y}_i - \mathbf{R}\mathbf{x}_i - \mathbf{t})^T (\mathbf{R}\boldsymbol{\Sigma}_{\mathrm{x}i}\mathbf{R}^T + \boldsymbol{\Sigma}_{\mathrm{y}i})^{-1} (\mathbf{y}_i - \mathbf{R}\mathbf{x}_i - \mathbf{t})$$

to a constrained optimization

$$\mathbf{T} = \underset{[\mathbf{R},\mathbf{t}]}{\operatorname{argmin}} \sum_{i=1}^{n} (\mathbf{x}_i - \mathbf{x}_i^*)^T \boldsymbol{\Sigma}_{\mathrm{x}i}^{-1} (\mathbf{x}_i - \mathbf{x}_i^*) + \sum_{i=1}^{n} (\mathbf{y}_i - \mathbf{y}_i^*)^T \boldsymbol{\Sigma}_{\mathrm{y}i}^{-1} (\mathbf{y}_i - \mathbf{y}_i^*)$$

$$\text{subject to:} \quad \mathrm{F}_i(\mathbf{x}_i^*, \mathbf{y}_i^*, \mathbf{R}, \mathbf{t}) = \mathbf{y}_i^* - \mathbf{R}\mathbf{x}_i^* - \mathbf{t} = 0$$

Generalized Total Least Squares (GTLS)

x_i* - true (unknown) data-point position
y_i* - true (unknown) model-point position

2. Linearize the constraints with a Taylor series centered at the measured (known) data

$$\mathrm{F}_i(\mathbf{x}_i^*, \mathbf{y}_i^*, \mathbf{R}, \mathbf{t}) \approx \mathrm{F}_{\mathrm{L}i}^k(\mathbf{x}_i, \mathbf{y}_i, \mathbf{d}\alpha, \mathbf{dt})$$
$$= \mathrm{F}_i^0(\mathbf{x}_i, \mathbf{y}_i, \mathbf{R}_k, \mathbf{t}_k) - \mathbf{r}_{\mathrm{y}i} + \mathbf{R}_k\mathbf{r}_{\mathrm{x}i} + \mathrm{skew}(\mathbf{R}_k\mathbf{x}_i)\mathbf{d}\alpha - \mathbf{dt} = 0$$

Note using: $\Delta\mathbf{R} \approx \mathbf{I} + \mathrm{skew}(\mathbf{d}\alpha)$ $\quad \mathbf{r}_{\mathrm{x}i} = \mathbf{x}_i - \mathbf{x}_i^*$ $\quad \mathbf{r}_{\mathrm{y}i} = \mathbf{y}_i - \mathbf{y}_i^*$

Copyright 2023 R. H. Taylor

Credit: Seth Billings

Engineering Research Center for Computer Integrated Surgical Systems and Technology

64

IMLP: Registration Phase

3. Apply the method of Lagrange multipliers to solve constrained optimization.

3a. Form the Lagrange function using the linearized constraints

$$\mathcal{L}(\mathbf{d}\alpha, \mathbf{dt}, \lambda) = \sum_{i=1}^{n} \mathbf{r}_{\mathrm{x}i}^T \boldsymbol{\Sigma}_{\mathrm{x}i}^{-1} \mathbf{r}_{\mathrm{x}i} + \sum_{i=1}^{n} \mathbf{r}_{\mathrm{y}i}^T \boldsymbol{\Sigma}_{\mathrm{y}i}^{-1} \mathbf{r}_{\mathrm{y}i} + \sum_{i=1}^{n} \lambda_i^T \, \mathrm{F}_{\mathrm{L}i}^k(\mathbf{x}_i, \mathbf{y}_i, \mathbf{d}\alpha, \mathbf{dt})$$

3b. Solve zero gradient w.r.t. the optimization parameters and the Lagrange multipliers

$$\mathbf{J}^T\boldsymbol{\Sigma}^{-1}\mathbf{J}\mathbf{dp} = -\mathbf{J}^T\boldsymbol{\Sigma}^{-1}\mathbf{f}^0$$

modified Gauss-Newton

$$\mathbf{dp} = \begin{bmatrix} \mathbf{d}\alpha \\ \mathbf{dt} \end{bmatrix} \quad \mathbf{f}^0 = \begin{bmatrix} \mathbf{f}_1^0 \\ \vdots \\ \mathbf{f}_n^0 \end{bmatrix} \quad \mathbf{J} = \begin{bmatrix} \mathrm{skew}(\mathbf{R}_k\mathbf{x}_1) & -\mathbf{I} \\ \vdots & \vdots \\ \mathrm{skew}(\mathbf{R}_k\mathbf{x}_n) & -\mathbf{I} \end{bmatrix} \quad \boldsymbol{\Sigma} = \left[\mathbf{F}_x^0 \boldsymbol{\Sigma}_{\mathrm{x}} \mathbf{F}_x^{0^T} + \boldsymbol{\Sigma}_{\mathrm{y}}\right]$$

$$\mathbf{F}_x^0 = \begin{bmatrix} -\mathbf{R}_k & & \\ & \ddots & \\ & & -\mathbf{R}_k \end{bmatrix} \quad \boldsymbol{\Sigma}_{\mathrm{x}} = \begin{bmatrix} \boldsymbol{\Sigma}_{\mathrm{x}1} & & \\ & \ddots & \\ & & \boldsymbol{\Sigma}_{\mathrm{x}n} \end{bmatrix} \quad \boldsymbol{\Sigma}_{\mathrm{y}} = \begin{bmatrix} \boldsymbol{\Sigma}_{\mathrm{y}1} & & \\ & \ddots & \\ & & \boldsymbol{\Sigma}_{\mathrm{y}n} \end{bmatrix}$$

4. Iteratively solve 3b by linear least squares until convergence.

$$\mathbf{R}_{k+1} = \mathbf{R}(\mathbf{d}\alpha)\mathbf{R}_k\,, \quad \mathbf{t}_{k+1} = \mathbf{t}_k + \mathbf{dt}$$

Copyright 2023 R. H. Taylor

Credit: Seth Billings

Engineering Research Center for Computer Integrated Surgical Systems and Technology

65

IMLP: Experiments

Credit: Seth Billings

- *Data Shape*: 100 noisy points + *outliers* simulated from a mesh model of a human hip
- *Model Shape*: point-cloud formed from the center points of the mesh triangles
- Random *initial misalignments* [30,60] mm and [30,60] degrees
- Target registration error (TRE) averaged over 300 *randomized trials* for each test case

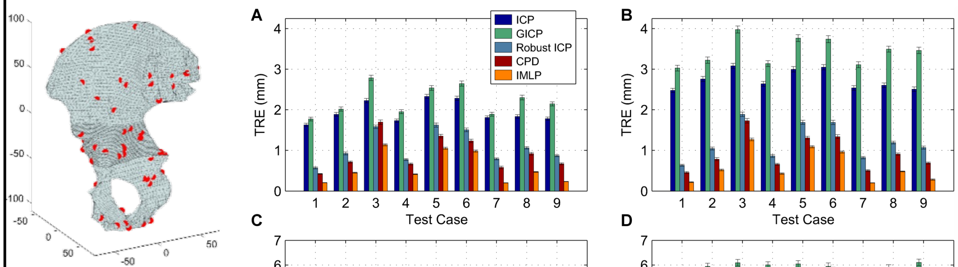

Alg	Average Runtime (sec.) by Test Case								
	1	2	3	4	5	6	7	8	9
ICP	0.009	0.009	0.010	0.009	0.010	0.009	0.009	0.009	0.009
IMLP-CP	0.015	0.016	0.019	0.016	0.020	0.019	0.015	0.017	0.015
IMLP-MD	0.068	0.078	0.093	0.079	0.097	0.093	0.067	0.079	0.069
GICP	-	-	-	-	-	-	-	-	-
CPD (2 cores)	3.465	4.346	4.336	3.864	4.340	4.374	4.238	4.650	4.484
IMLP	0.068	0.082	0.102	0.078	0.103	0.099	0.067	0.084	0.073

67

IMLP: Experiments

Credit: Seth Billings

- Data Shape: 100 noisy points simulated from a mesh model of a human femur
- Model Shape: point-cloud formed from the center points of the mesh triangles
- Random initial misalignments [10,20] mm and [10,20] degrees
- Target registration error (TRE) averaged over 300 randomized trials for each test case

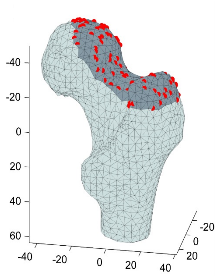

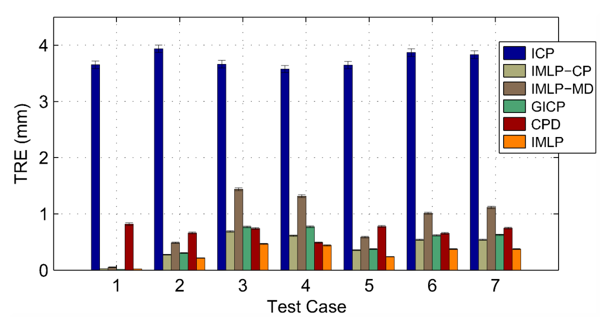

Alg.	Failure Rate (%) by Test Case						
	1	2	3	4	5	6	7
ICP	15.0	10.7	17.3	13.7	14.7	18.7	16.3
IMLP-CP	4.7	2	5.3	4.3	4.3	4.3	4.0
IMLP-MD	6.0	3.3	7.3	5.3	7.0	6.7	5.3
GICP	6.0	4.3	8.3	6.3	6.0	5.3	4.7
CPD	0.0	0.0	0.0	0.0	0.0	0.3	0.3
IMLP	6.0	3.0	7.0	5.0	6.0	6.3	5.0

68

Credit: Seth Billings

IMLP: Experiments

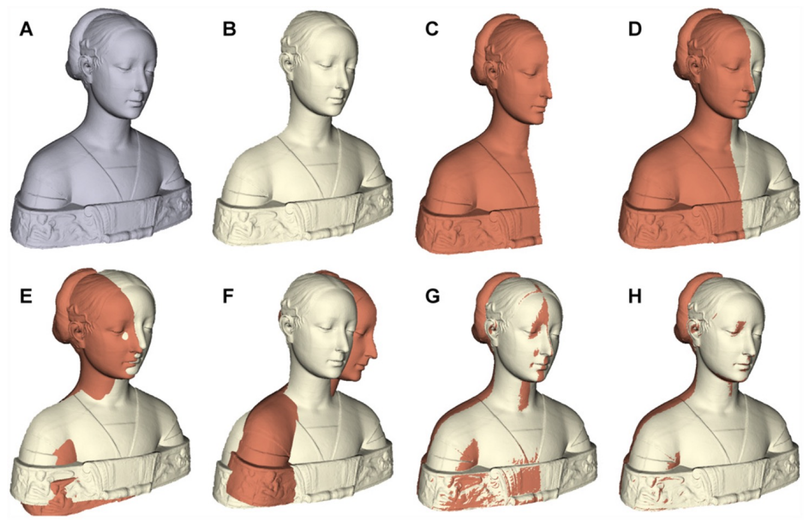

Fig 9. Registration of shapes having partial overlap. (Experiment 7). (A): The statue Laurana sub-divided into (B): front and (C): right half-sections, such that (D): a 50% overlap exists between the two sub-shapes. The sub-shapes were (E): misaligned by 10 mm and 10 degrees in a random direction and then registered using (F): CPD [20], (G): GICP [11], and (H): the proposed IMLP algorithm. Sub-figures (E-H) show the initial misalignment and the final registered alignments of the two shapes for the 6th randomized trial of Experiment 7, which involved 10 randomized trials in total.

doi:10.1371/journal.pone.0117688.g009

69

Iterative Most Likely Oriented Point (IMLOP)

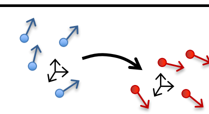

- **Matching Phase**:

  for each oriented point in the source shape, find the most likely oriented point on the target shape

$$\boldsymbol{y_i} = \mathrm{C}_{\mathrm{MLP}}(T(\boldsymbol{x_i}), \Psi) = \underset{\boldsymbol{y} \in \Psi}{\operatorname{argmax}} \, f_{\mathrm{match}}(T(\boldsymbol{x_i}), \boldsymbol{y})$$

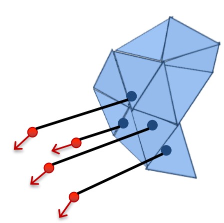

- **Registration Phase:**

  compute transformation to maximize the likelihood (i.e. minimize negative log-likelihood) of oriented point matches

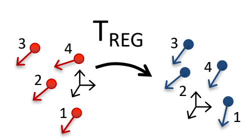

$$T = \underset{T}{\operatorname{argmin}} \left(\frac{1}{2\sigma^2} \sum_{i=1}^{n} \|\boldsymbol{y}_{\mathrm{p}\boldsymbol{i}} - T(\boldsymbol{x}_{\mathrm{p}\boldsymbol{i}})\|_2^2 - k \sum_{i=1}^{n} \boldsymbol{y}_{\mathrm{n}\boldsymbol{i}}{}^T R \boldsymbol{x}_{\mathrm{n}\boldsymbol{i}} \right)$$

S. Billings and R. H. Taylor, "Iterative Most Likely Oriented Point Registration", ***in Medical Image Computing and Computer-Assisted Interventions (MICCAI)*****, Boston, October, 2014.**

Copyright 2023 R. H. Taylor

Engineering Research Center for Computer Integrated Surgical Systems and Technology

71

Sources of Orientation Data

Video

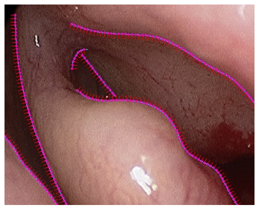

X-Ray

Shape Models

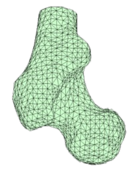

Tracked Pointer

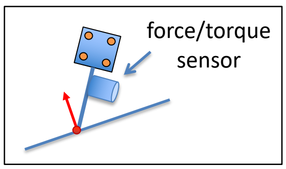

Oriented Fiducials

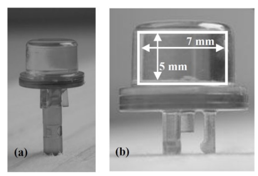

Ultrasound

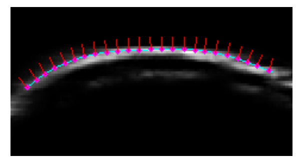

Figures: http://www.ndigital.com/wp-content/uploads/2013/09/4col_polarisvicra1.png; *The Essential Physics of Medical Imaging, 3rd ed.*; http://www.infotech.edu/wp-content/uploads/2013/01/L.A.B.-Look-At-Baby-3D-Ultrasound-Tests-Ultrasound-Technicians-bw-300x225.jpg; http://i00.i.aliimg.com/photo/v0/105832128/CT_Scan_equipment.jpg; http://goodpixgallery.com/dl/?i=835588; Liu X, Cevikalp H, Fitzpatrick JM (2003) Marker orientation in fiducial registration. In: Sonka M, Fitzpatrick JM, editors. SPIE, Medical Imaging 2003: Image Processing. Vol. 5032. pp. 1176–1185.

Copyright 2023 R. H. Taylor

Credit: Seth Billings

72

Experiments

Performance comparison of IMLOP vs. ICP was made through a simulation study using a human femur surface mesh segmented from CT imaging.

- source shape created by randomly sampling points from the mesh surface (10, 20, 35, 50, 75, and 100 points tested)
- Gaussian [wrapped Gaussian] noise added to the source points (0, 0.5, 1.0, and 2.0 mm [degrees] tested)
- Applied random misalignment of [10,20] mm / degrees
- 300 trials performed for each sample size / noise level
- Registration accuracy (TRE) evaluated using 100 validation points randomly sampled from the mesh
- Registration failures automatically detected using threshold on final residual match errors

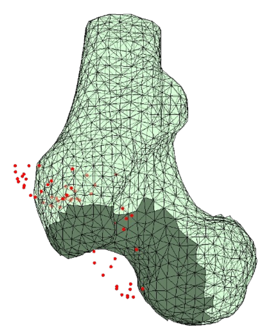

Example source point cloud sampled from dark region of target mesh.

ICP: threshold on position residuals only
IMLOP: threshold on position & orientation residuals

S. Billings and R. H. Taylor, "Iterative Most Likely Oriented Point Registration", *in Medical Image Computing and Computer-Assisted Interventions (MICCAI)*, Boston, October, 2014.

Copyright 2023 R. H. Taylor

74

Average TRE of successful registrations and registration failure rates across all sample sizes for noise levels of 1 (A) and 2 (B) mm [degrees].

Registration failure threshold set to twice the noise level for both position and orientation.

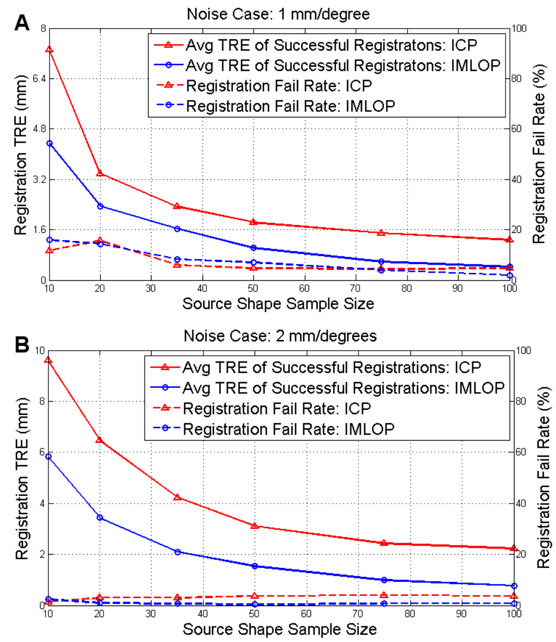

S. Billings and R. H. Taylor, "Iterative Most Likely Oriented Point Registration", *in Medical Image Computing and Computer-Assisted Interventions (MICCAI)*, Boson, October, 2014. (accepted).

Copyright 2023 R. H. Taylor

Engineering Research Center for Computer Integrated Surgical Systems and Technology

75

Experiments

Results from 300 trials within a single sample size (75 points) and noise level (1.0 mm [degree]). NOTE: improved accuracy and failure detection capability for IMLOP.

ICP **IMLOP**

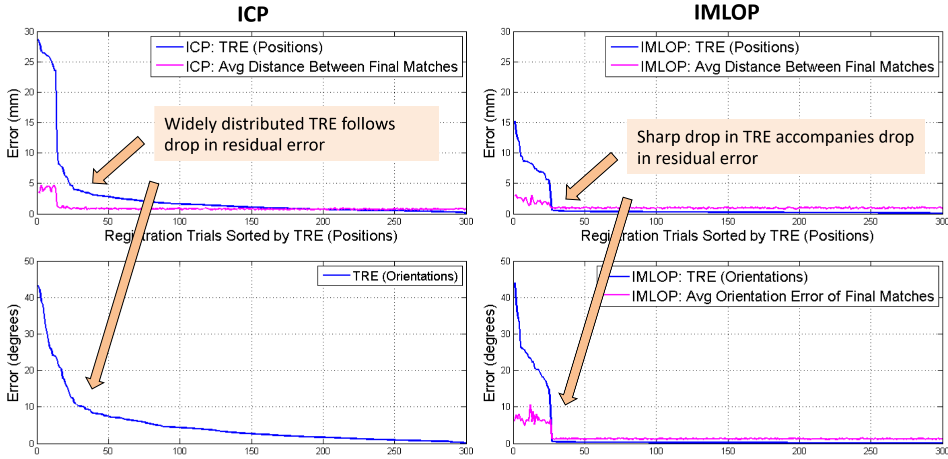

S. Billings and R. H. Taylor, "Iterative Most Likely Oriented Point Registration", *in Medical Image Computing and Computer-Assisted Interventions (MICCAI)*, Boston, October, 2014. (accepted).

Copyright 2023 R. H. Taylor

Engineering Research Center for Computer Integrated Surgical Systems and Technology

76

Generalized IMLOP Results

- Extends IMLOP to account for anisotropic measurement error distributions
  - Model orientations with Kent distributions
  - Model positions with Gaussian distributions
- Simulation results for 50 samples shown below

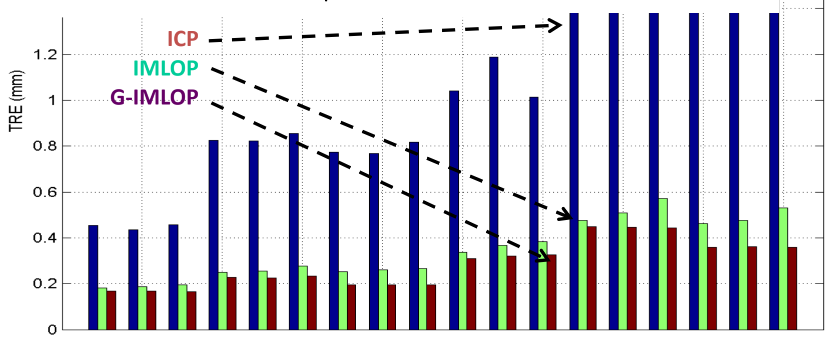

S. Billings and R. Taylor, "Generalized Iterative Most-Likely Oriented Point (G-IMLOP) Registration", *Int. J. Computer Assisted Radiology and Surgery*, 8(10) p.1213-1226, 2015.

Copyright 2023 R. H. Taylor

Engineering Research Center for Computer Integrated Surgical Systems and Technology

77

Experiments: TRE for Rejected and Non-Rejected Registrations

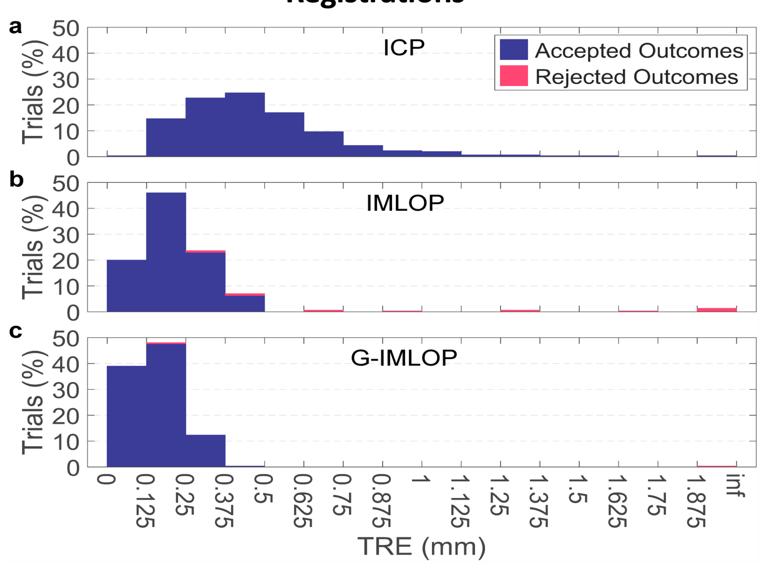

[S. Billings and R. Taylor, "Generalized Iterative Most-Likely Oriented Point (G-IMLOP) Registration", Int. J. Computer Assisted Radiology and Surgery, p. Accepted 2015.

Copyright 2023 R. H. Taylor

Engineering Research Center for Computer Integrated Surgical Systems and Technology

78

Ultrasound-assisted Registration

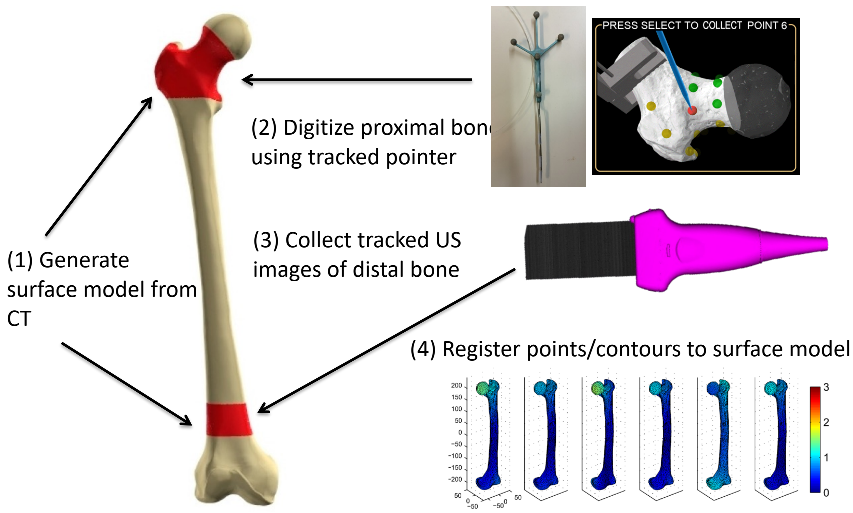

S. Billings, H. J. Kang, A. Cheng, E. Boctor, P. Kazanzides, and R. Taylor, "Minimally invasive registration for computer-assisted orthopedic surgery: combining tracked ultrasound and bone surface points via the P-IMLOP algorithm", Int. J. Computer Assisted Radiology and Surgery, p. (epub ahead of print), 2015. http://dx.doi.org/10.1007/s11548-015-1188-z DOI 10.1007/s11548-015-1188-z

Copyright 2023 R. H. Taylor

79

Intensity-based methods

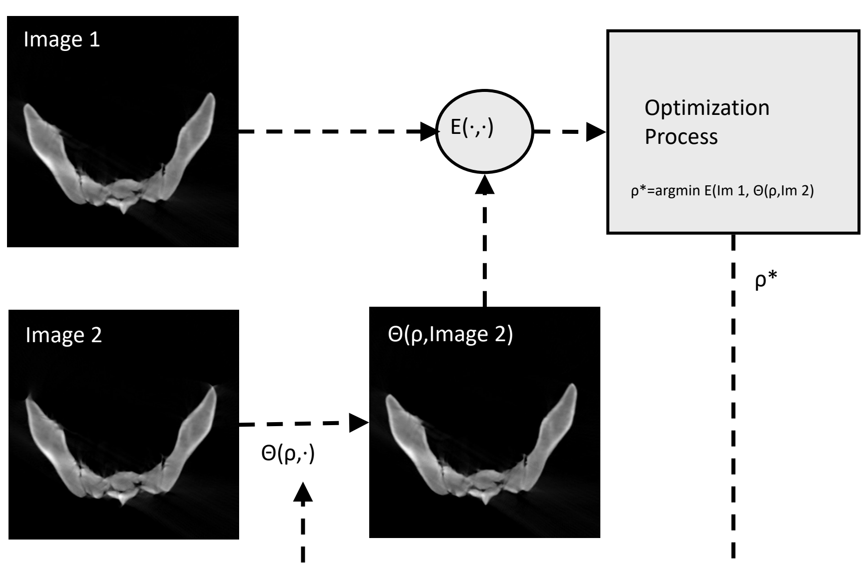

Copyright 2023 R. H. Taylor

80

Basic Idea of Intensity-Based 2D/3D Registration

- Assumes a pre-op CT is available
- Simulate many C-Arm images and choose the most similar to the intraoperative image
- Solves the following optimization problem:

$$\operatorname*{argmin}_{\theta \in SE(3)} \mathcal{S}(I_{\text{Intra-Op}}, \mathcal{P}(\theta, I_{\text{CT}}))$$

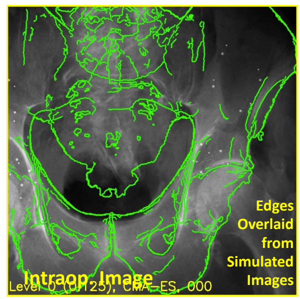

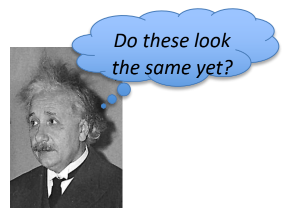

Slide credit: Robert Grupp

Copyright 2023 R. H. Taylor

Engineering Research Center for Computer Integrated Surgical Systems and Technology

81

Intensity-based methods

- Typically performed between images
- The “features” in this case are the intensities associated with pixels (2D) or voxels (3D) in the images.
- General framework:

$$\vec{\rho}^{\,*} = \min_{\vec{\rho}} E\left(Image_1, \Theta\left(\vec{\rho}, Image_2\right)\right)$$

- Methods differ mostly in choice of transformation function *Θ(·)* and Energy function *E(·,·),*

Copyright 2023 R. H. Taylor

Engineering Research Center for Computer Integrated Surgical Systems and Technology

82

Typical energy functions
(not an exhaustive list)

Normalized image subtraction

$$E(\mathrm{Im}_1,\mathrm{Im}_2)=\sum_{\bar{k}}\frac{\left|\mathrm{Im}_1[\bar{k}]-\mathrm{Im}_2[\bar{k}]\right|}{\max_{\bar{j}}\left(\left|\mathrm{Im}_1[\bar{j}]-\mathrm{Im}_2[\bar{j}]\right|\right)}$$

Normalized cross correlation (NCC)

$$E(\mathrm{Im}_1,\mathrm{Im}_2)=\frac{\sum_{\bar{k}}\left(\mathrm{Im}_1[\bar{k}]-avg(\mathrm{Im}_1)\right)\left(\mathrm{Im}_2[\bar{k}]-avg(\mathrm{Im}_2)\right)}{\sqrt{\sum_{\bar{k}}\left(\mathrm{Im}_1[\bar{k}]-avg(\mathrm{Im}_1)\right)^2}\sqrt{\sum_{\bar{k}}\left(\mathrm{Im}_2[\bar{k}]-avg(\mathrm{Im}_2)\right)^2}}$$

Mutual information

$$E(\mathrm{Im}_1,\mathrm{Im}_2)=\sum_{p\in\mathrm{Im}_1\, q\in\mathrm{Im}_2}\Pr(p,q)\log\Pr(p,q)-\Pr_{\mathrm{Im}_1}(p)\log\Pr_{\mathrm{Im}_1}(p)-\Pr_{\mathrm{Im}_2}(q)\log\Pr_{\mathrm{Im}_2}(q)$$

Copyright 2023 R. H. Taylor

Mutual Information

- First proposed independently in 1995 by Collignon and Viola & Wells.
- Very widely practiced
- Is able to co-register images with very different sensor modalities so long as there is a stable relationship between intensities in one modality with those in another
- Many “flavors” and variations

Copyright 2023 R. H. Taylor

Mutual Information

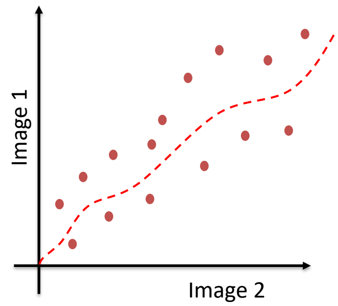

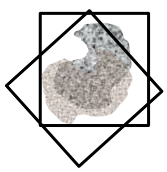

- The key idea is that the values of pixels in one image can predict the values of the pixels in the other image, even if the images come from different sensors
- The strength of this prediction will increase as the images become better aligned

Copyright 2023 R. H. Taylor

Engineering Research Center for Computer Integrated Surgical Systems and Technology

85

Mutual Information

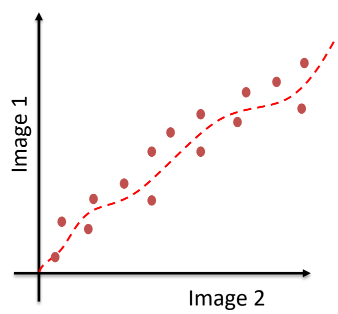

- The key idea is that the values of pixels in one image can predict the values of the pixels in the other image, even if the images come from different sensors
- The strength of this prediction will increase as the images become better aligned

Copyright 2023 R. H. Taylor

Engineering Research Center for Computer Integrated Surgical Systems and Technology

86

Mutual Information

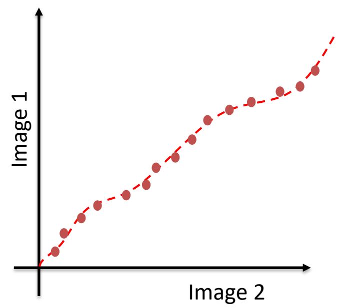

- The key idea is that the values of pixels in one image can predict the values of the pixels in the other image, even if the images come from different sensors
- The strength of this prediction will increase as the images become better aligned

Copyright 2023 R. H. Taylor

Mutual Information

Entropy

$$H(a) = \Pr(a)\log\Pr(a)$$

$$H(a,b) = \Pr(a,b)\log\Pr(a,b)$$

Mutual Information (Viola & Wells '95, Colligen '95)

$$Similarity(A,B) = H(A) + H(B) - H(A,B)$$

Normalized mutual information (Maes *et al.* '97)

$$Similarity(A,B) = \frac{H(A)+H(B)}{H(A,B)}$$

Objective function

$$\mathrm{E}(\mathrm{Im}_1,\mathrm{Im}_2) = -Similarity(\mathrm{Im}_1,\mathrm{Im}_2)$$

Copyright 2023 R. H. Taylor

Rigid 3D/2D Registration

Ofri Sadowsky

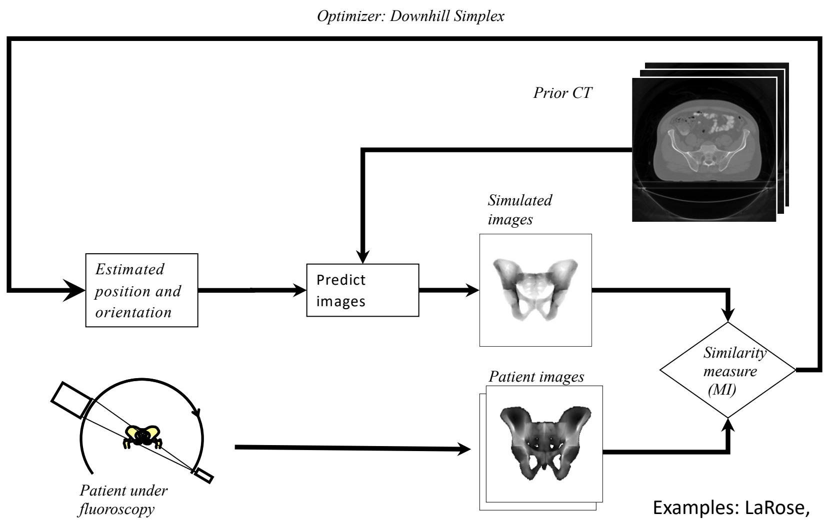

Examples: LaRose, Zollei, …

Copyright 2023 R. H. Taylor

89

ciis

A clinical example (periacetublar osteotomy)

Problem: Acetabular Dysplasia

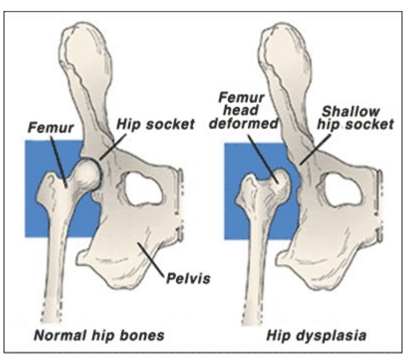

Image Source: ouh.nhs.uk

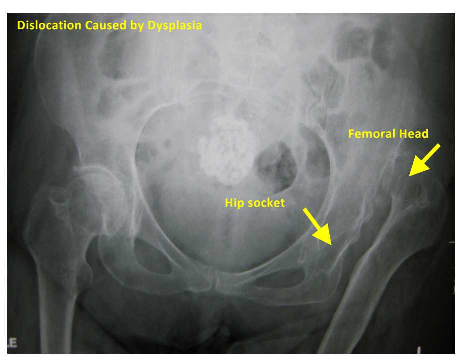

Image Source: James Heilman, MD

Slide credit: Robert Grupp

Copyright 2023 R. H. Taylor

91

ciis

A clinical example (periacetublar osteotomy)

One Solution: Periacetabular Osteotomy (PAO)

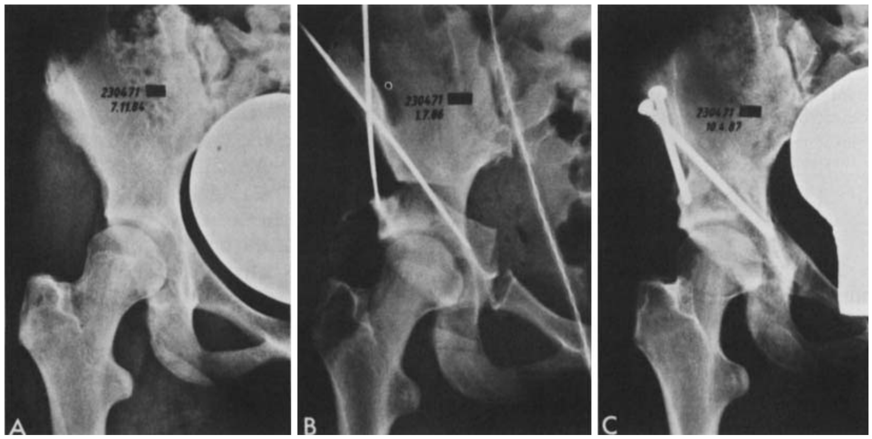

Image Source: Ganz 1988

Copyright 2023 R. H. Taylor

Slide credit: Robert Grupp

92

ciis

A clinical example (periacetublar osteotomy)

Goal: Automatic visualization and guidance

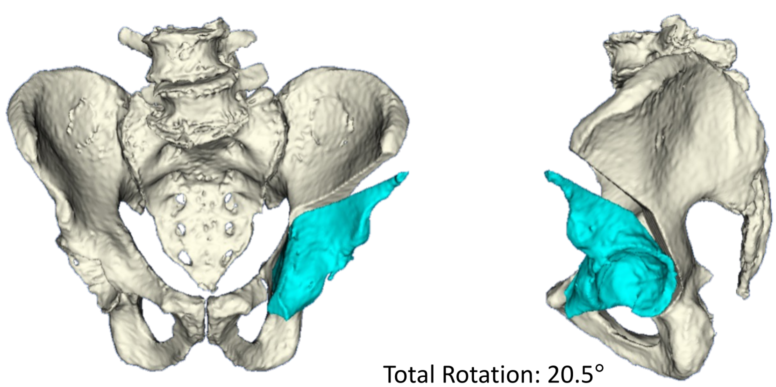

Total Rotation: 20.5°
Anterior/Posterior Rotation: 3.7°
Left/Right Rotation: 16.3°
Inferior/Superior Rotation: 12.5°

Slide credit: Robert Grupp

Copyright 2023 R. H. Taylor

93

Movement of the Osteotomy Fragment is Challenging

Slide credit: Robert Grupp

Copyright 2023 R. H. Taylor

Engineering Research Center for Computer Integrated Surgical Systems and Technology

94

One Approach for Computer-Assistance: Optical Tracking Devices

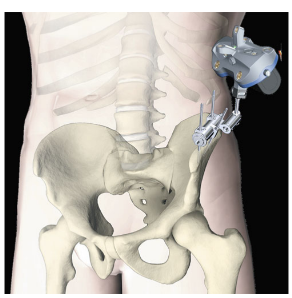

Source: Stiehl and Thornberry, 2016

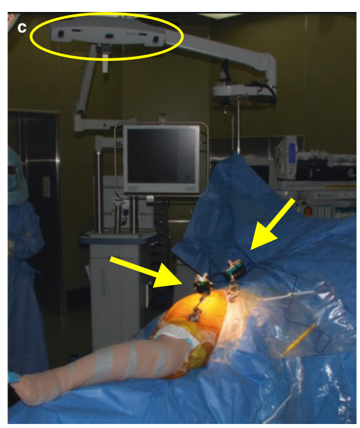

Source: Sugano, CAOS for Hip and Knee, 2018

Slide credit: Robert Grupp

Copyright 2023 R. H. Taylor

Engineering Research Center for Computer Integrated Surgical Systems and Technology

95

Intraoperative Fluoroscopy is Available

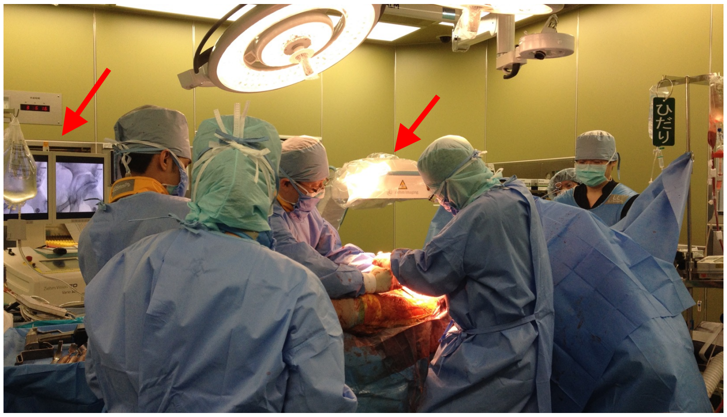

Chapter 4: Pose Estimation Using Fluoroscopy

Slide credit: Robert Grupp

Copyright 2023 R. H. Taylor

Engineering Research Center for Computer Integrated Surgical Systems and Technology

96

Intraoperative X-Ray Imaging with Mobile C-Arm

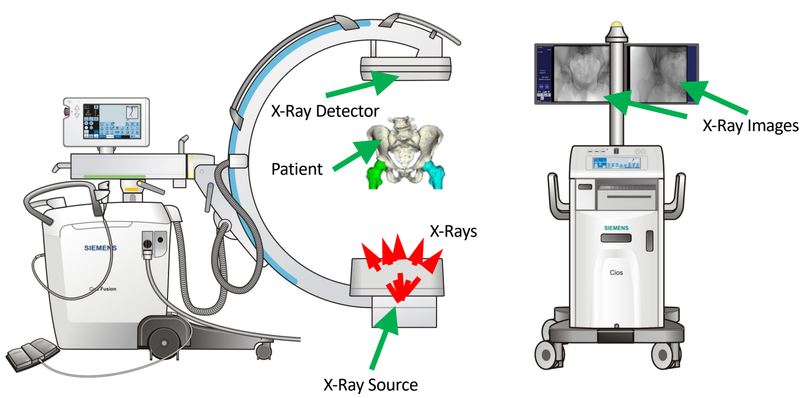

C-Arm Image Source: Siemens CIOS Fusion Manual

Chapter 4: Pose Estimation Using Fluoroscopy

Slide credit: Robert Grupp

Copyright 2023 R. H. Taylor

Engineering Research Center for Computer Integrated Surgical Systems and Technology

97

Proposed Workflow

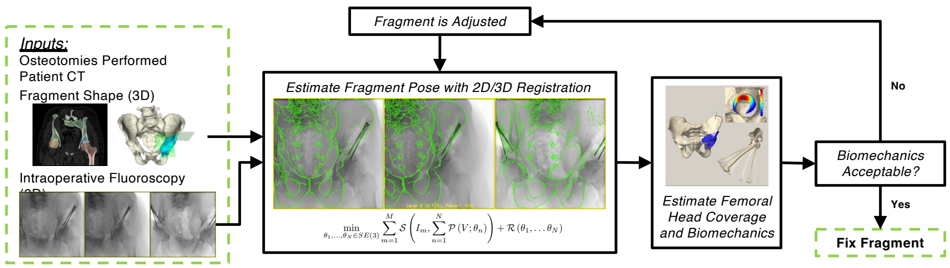

Chapter 4: Pose Estimation Using Fluoroscopy

Copyright 2023 R. H. Taylor

ciis

3D-2D Registration of Osteotomy Fragments

BIGSS

$$\underset{\theta_1,\ldots,\theta_N \in SE(3)}{\arg\min} \sum_{m=1}^{M} \mathcal{S}\left(I_m, \sum_{n=1}^{N} \mathcal{P}_m\left(I_{CT};\theta_n\right)\right)$$

Fixed Images with Moving Image Edges

Moving Images

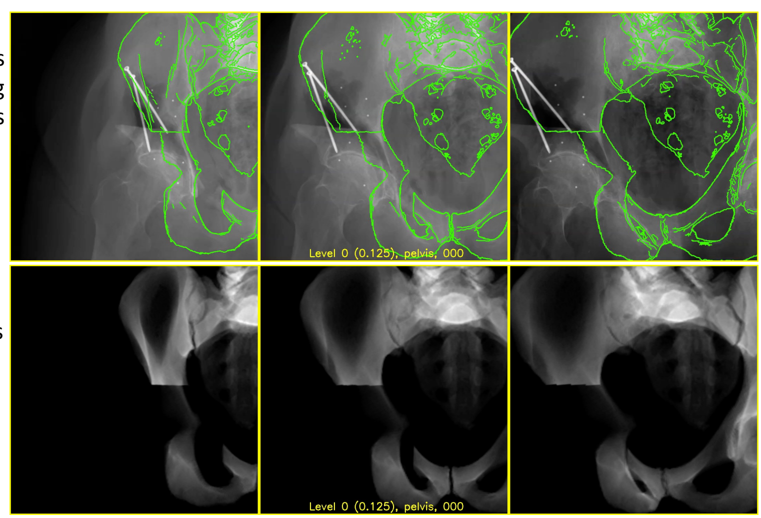

R. Grupp, R. Murphy, M. Armand, R. Taylor

Copyright 2023 R. H. Taylor

Slide credit: Robert Grupp

3D-2D Registration of Osteotomy Fragments

- Compute the Sobel derivatives in the X and Y directions of the two input images:

$$\nabla_X I_1,\ \nabla_X I_2,\ \nabla_Y I_1,\ \nabla_Y I_2$$

- Compute NCC between the corresponding gradient images:

$$\mathcal{S}(I_1, I_2) = NCC(\nabla_X I_1, \nabla_X I_2) + NCC(\nabla_Y I_1, \nabla_Y I_2)$$

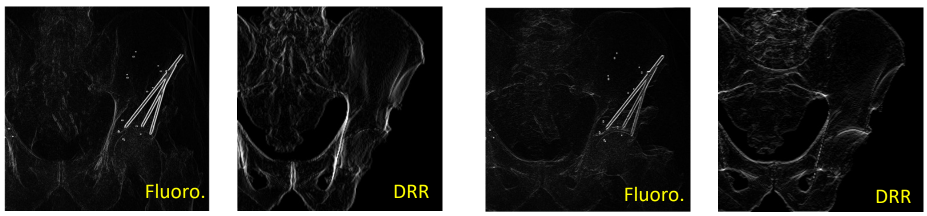

$\nabla_X I_1$ $\nabla_X I_2$ $\nabla_Y I_1$ $\nabla_Y I_2$

R. Grupp, R. Murphy, M. Armand, R. Taylor

Copyright 2023 R. H. Taylor Slide credit: Robert Grupp Engineering Research Center for Computer Integrated Surgical Systems and Technology

100

Initialize Using a Nominal AP View?

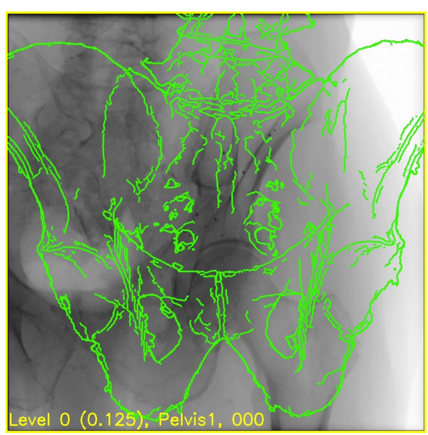

Chapter 4: Pose Estimation Using Fluoroscopy

Slide credit: Robert Grupp

Copyright 2023 R. H. Taylor Engineering Research Center for Computer Integrated Surgical Systems and Technology

101

Too Many Local Minima!

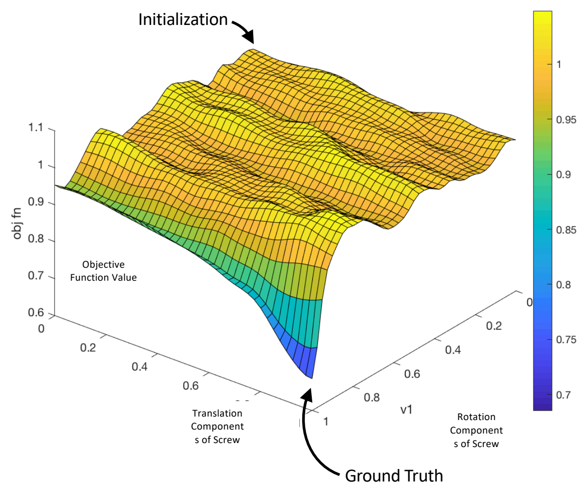

Chapter 4: Pose Estimation Using Fluoroscopy

Copyright 2023 R. H. Taylor

Engineering Research Center for Computer Integrated Surgical Systems and Technology

102

Use a Single Landmark to Initialize Registration

- Assume the pelvis is in an AP orientation – this may be computed preoperatively
- Manually annotate a single landmark to recover translation

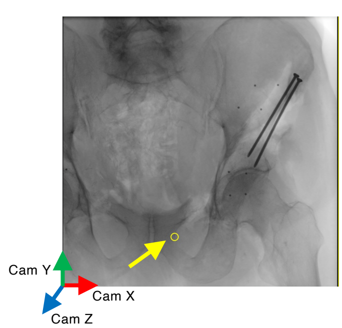

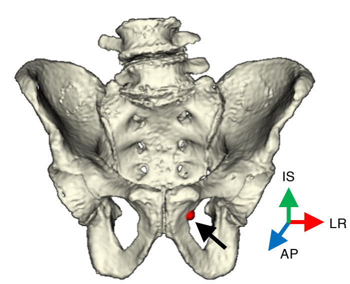

Chapter 4: Pose Estimation Using Fluoroscopy

Slide credit: Robert Grupp

Copyright 2023 R. H. Taylor

Engineering Research Center for Computer Integrated Surgical Systems and Technology

103

Example of a Single Landmark Initialization

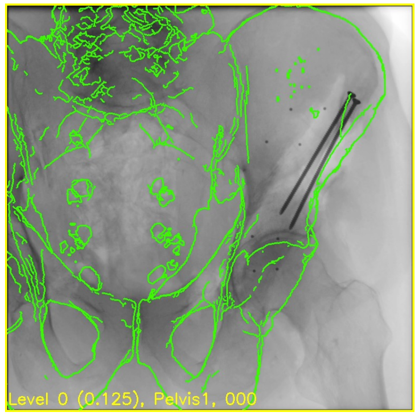

Chapter 4: Pose Estimation Using Fluoroscopy

Copyright 2023 R. H. Taylor

Slide credit: Robert Grupp

Engineering Research Center for Computer Integrated Surgical Systems and Technology

104

Automatically Initialize Second and Third Views

- Constrain C-arm motion to orbital rotation
- Perform an exhaustive search over $\pm 90°$ in $1°$ increments

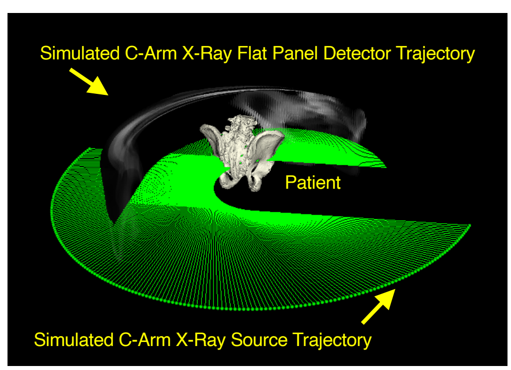

Chapter 4: Pose Estimation Using Fluoroscopy

Copyright 2023 R. H. Taylor

Slide credit: Robert Grupp

Engineering Research Center for Computer Integrated Surgical Systems and Technology

105

Example Initializations From Orbital Search

View #2

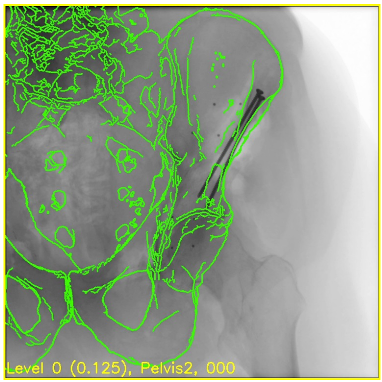

View #3

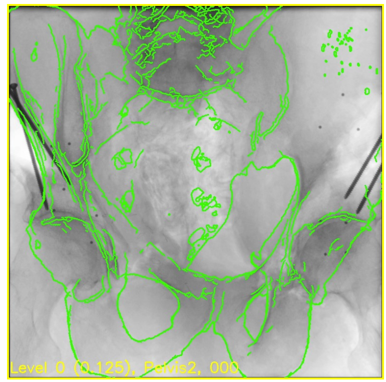

Chapter 4: Pose Estimation Using Fluoroscopy

Slide credit: Robert Grupp

Copyright 2023 R. H. Taylor

Engineering Research Center for Computer Integrated Surgical Systems and Technology

106

Automatic Landmark-Based Initialization

- Train a CNN to recognize approximate landmark positions in x-ray images

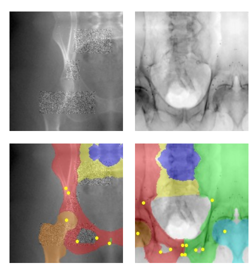

- Use landmark-based 2D-3D registration to initialize registration
- Combine landmark and intensity objective functions
- Use segmentation labels to ignore intensities of irrelevant anatomy

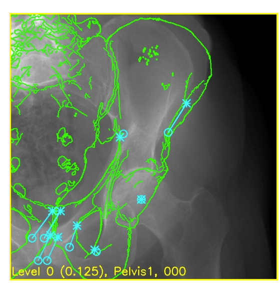

Images: Robert Grupp

Copyright 2023 R. H. Taylor

Engineering Research Center for Computer Integrated Surgical Systems and Technology

107

Why Not Simultaneously Use Intensities and Features?

- Registration objective function:

$$\min_{\theta_P,\theta_{LF},\theta_{RF}\in SE(3)} \lambda\mathcal{S}\left(\mathcal{P}\left(\theta_P,\theta_{LF},\theta_{RF}\right),I\right)+(1-\lambda)\,\mathcal{R}\left(\theta_P,\theta_{LF},\theta_{RF}\right)$$

Image Similarity Term

Regularization Term

- Usually, regularization penalizes the amount of rotation and translation away from initialization
- Why not directly include the landmark re-projection as regularization?

$$\mathcal{R}\left(\theta_P\right)=\frac{1}{2\sigma_\ell^2}\sum_{l=1}^{N_L}\left\|\mathcal{P}\left(p_{\mathrm{3D}}^{(l)};\theta_P\right)-p_{\mathrm{2D}}^{(l)}\right\|_2^2$$

- Can also think of this as running landmark registration and regularizing on image appearance

Chapter 6: Automatic and Robust Registration

Copyright 2023 R. H. Taylor Slide credit: Robert Grupp

Engineering Research Center for Computer Integrated Surgical Systems and Technology

108

Include Landmark Reprojection Into Objective Function

- Landmarks Detected in 2D are Shown as Cyan Circles
- Landmarks Projected from 3D are Shown as Cyan Asterisks *
- Cyan Lines Indicate Correspondence
- The Initial Pose Aligns the 2D and 3D Left Femoral Head Centers

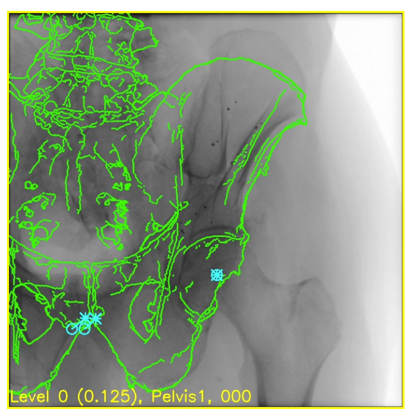

Chapter 6: Automatic and Robust Registration

Copyright 2023 R. H. Taylor

Engineering Research Center for Computer Integrated Surgical Systems and Technology

109

Objective Function When Combining Landmark Re-Projection

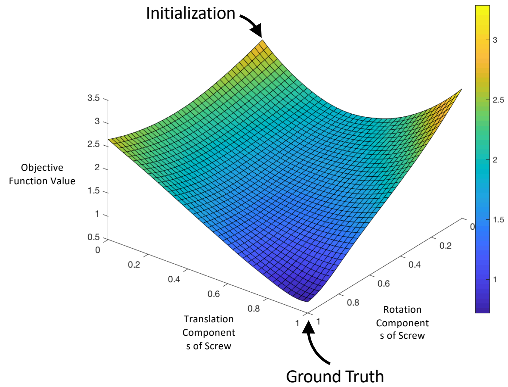

Line between initialization and ground truth is the *SE*(3) screw motion

Chapter 6: Automatic and Robust Registration

Slide credit: Robert Grupp

Copyright 2023 R. H. Taylor

110

Challenge: Narrow Capture Range

Narrow Capture Range

- Local minima of conventional hand-crafted similarity function, such as Grad-NCC
- Requires the initialization close to the ground truth

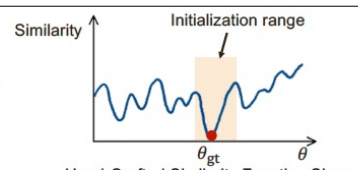

Hand-Crafted Similarity Function Shape

Conventional Intensity-based 2D/3D Registration Strategy:
- CMAES + Patch-based Grad-NCC[25]

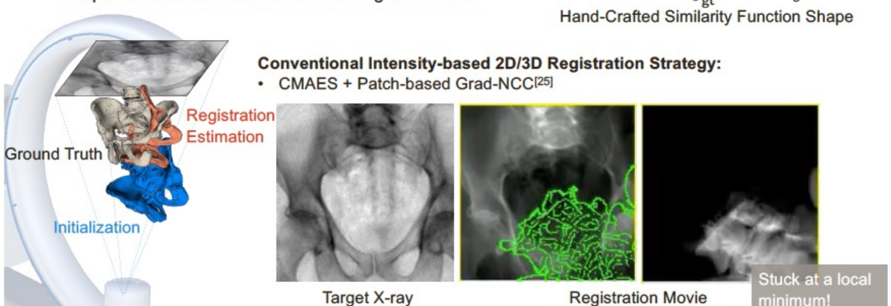

Target X-ray

Registration Movie

[25] Grupp, R.B., Armand, M. and Taylor, R.H., 2018. Patch-based image similarity for intraoperative 2D/3D pelvis registration during periacetabular osteotomy. In CARE Workshop of MICCAI 2018.

109

Slide Credit: Cong Gao, *Fluoroscopic Navigation for Robot-Assisted Orthopedic Surgery*, PhD Dissertation Defense, August 2022

Copyright 2023 R. H. Taylor

111

Can CNNs Help?

Pose Regression Methods

Limitations:

- Learning a mapping function from 2D projections is **an ill-posed problem**, which is prone to **strongly overfit to training domain**
- **Direct pose regression is unconstrained**, which can change dramatically if the input image appearance has a tiny difference

Target X-ray DRR

High-level Prototype

[26] Miao, S., Wang, Z.J. and Liao, R., 2016. A CNN regression approach for real-time 2D/3D registration. IEEE transactions on medical imaging, 35(5), pp.1352-1363.

110

Slide Credit: Cong Gao, *Fluoroscopic Navigation for Robot-Assisted Orthopedic Surgery*, PhD Dissertation Defense, August 2022

Copyright 2023 R. H. Taylor

Engineering Research Center for Computer Integrated Surgical Systems and Technology

112

Can CNNs Help?

A More Desired Solution

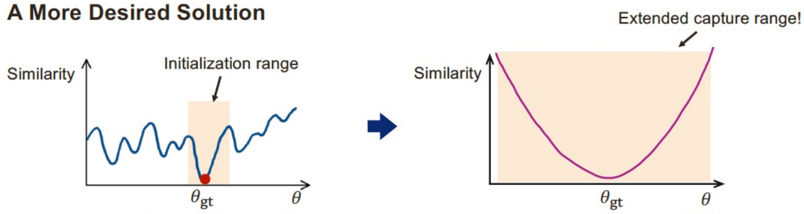

Hand-Crafted Similarity Function Shape

Network Similarity Function Shape

Traditional DRR Projector is not Differentiable!

- Oversized system matrix $A(\theta)$ to fit in memory
- Conventional optimization strategies are numeric-based methods, such as CMAES

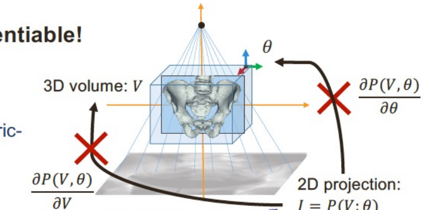

[27] Hansen, N., Müller, S.D. and Koumoutsakos, P., 2003. Reducing the time complexity of the derandomized evolution strategy with covariance matrix adaptation (CMA-ES). Evolutionary computation, 11(1), pp.1-18.

111

Slide Credit: Cong Gao, *Fluoroscopic Navigation for Robot-Assisted Orthopedic Surgery*, PhD Dissertation Defense, August 2022

Copyright 2023 R. H. Taylor

Engineering Research Center for Computer Integrated Surgical Systems and Technology

113

Differentiable DRR Operator (Gao)

ProST -- Differentiable DRR Operator

Spatial Sampling Grid: G

- Follows projection geometry

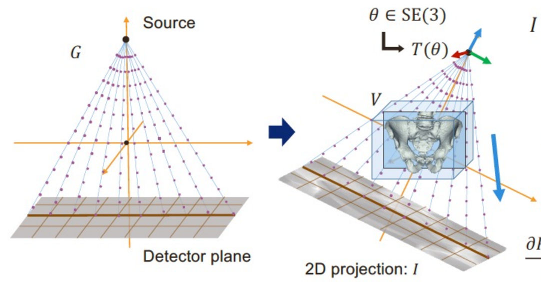

Given a pose parameter θ and 3D volume V as input, the DRR projection is:

$$I = P(V,\theta)$$
$$= \mathrm{sum}(\mathrm{interp}(V, T(\theta)G))$$

Linear transformation
Linear interpolation
Summation along the projection direction

Breakthrough:

$\frac{\partial P(V,\theta)}{\partial \theta}$ $\frac{\partial P(V,\theta)}{\partial V}$ are differentiable!

[28] **Gao, C.**, Liu, X., Gu, W., Killeen, B., Armand, M., Taylor, R., & Unberath, M. (2020, October). Generalizing spatial transformers to projective geometry with applications to 2D/3D registration. In International Conference on Medical Image Computing and Computer-Assisted Intervention (pp. 329-339). Springer, Cham.

JOHNS HOPKINS WHITING SCHOOL of ENGINEERING · LABORATORY FOR Computational Sensing + Robotics · BIGSS · ARCADE 112

Slide Credit: Cong Gao, *Fluoroscopic Navigation for Robot-Assisted Orthopedic Surgery*, PhD Dissertation Defense, August 2022

Copyright 2023 R. H. Taylor

Engineering Research Center for Computer Integrated Surgical Systems and Technology

114

ProST -- Projective Spatial Transformers (Gao)

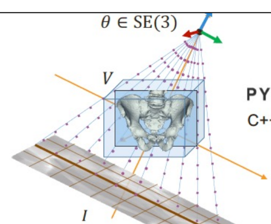

PYTORCH
C++, CUDA backend

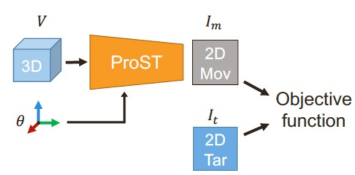

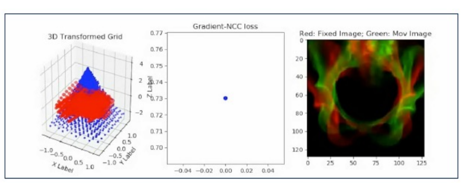

Example registration using Grad-NCC similarity, optimized by PyTorch built-in SGD optimizer

How do we learn a better similarity function?

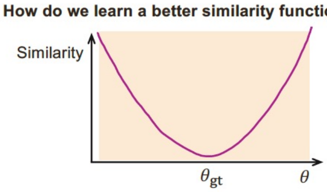

Network Similarity Function Shape

JOHNS HOPKINS WHITING SCHOOL of ENGINEERING · LABORATORY FOR Computational Sensing + Robotics · BIGSS · ARCADE 113

Slide Credit: Cong Gao, *Fluoroscopic Navigation for Robot-Assisted Orthopedic Surgery*, PhD Dissertation Defense, August 2022

Copyright 2023 R. H. Taylor

Engineering Research Center for Computer Integrated Surgical Systems and Technology

115

ProST – 2D/3D Registration Pipeline (Gao)

Target Similarity Function -- Geodesic Loss

- A convex objective function with respect to SE(3) pose parameters

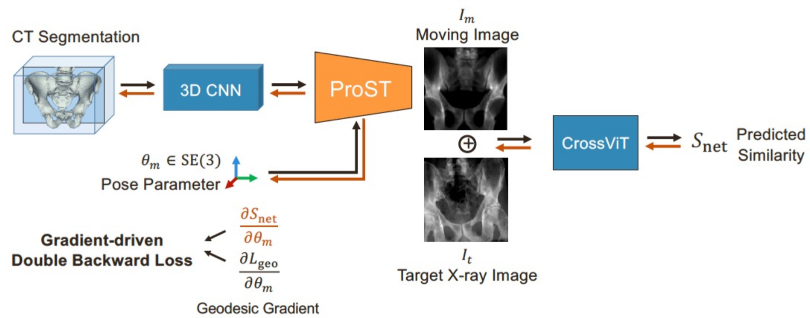

JOHNS HOPKINS WHITING SCHOOL of ENGINEERING · Laboratory for Computational Sensing + Robotics · BIGSS · ARCADE 114

Slide Credit: Cong Gao, *Fluoroscopic Navigation for Robot-Assisted Orthopedic Surgery*, PhD Dissertation Defense, August 2022

Copyright 2023 R. H. Taylor

Engineering Research Center for Computer Integrated Surgical Systems and Technology

116

ProST – 2D/3D Registration Pipeline (Gao)

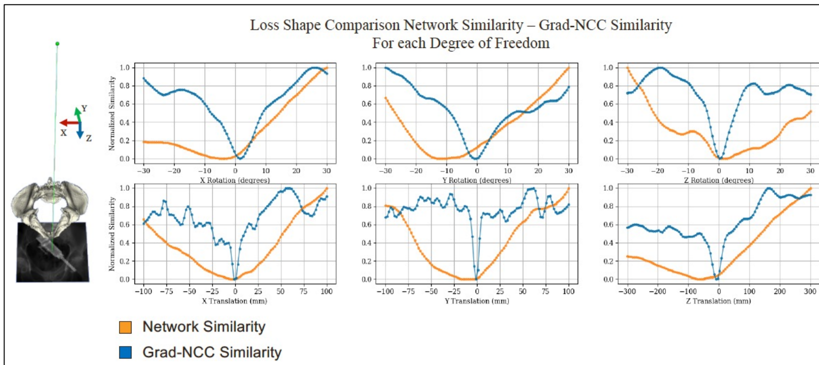

JOHNS HOPKINS WHITING SCHOOL of ENGINEERING · Laboratory for Computational Sensing + Robotics · BIGSS · ARCADE 117

Slide Credit: Cong Gao, *Fluoroscopic Navigation for Robot-Assisted Orthopedic Surgery*, PhD Dissertation Defense, August 2022

Copyright 2023 R. H. Taylor

Engineering Research Center for Computer Integrated Surgical Systems and Technology

118

ProST – 2D/3D Registration Pipeline (Gao)

- Our pipeline was trained using 19 CT scans, evaluated on 1,000 synthetic X-rays and 200 real X-rays

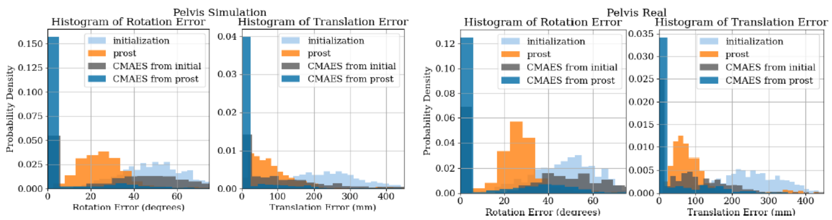

Success Rate (%): Mean Target Registration Error < 10 mm

	Simulation	Real
CMAES from Initialization	32.6	36.0
CMAES from ProST Registration	**82.6**	**73.2**

JOHNS HOPKINS WHITING SCHOOL of ENGINEERING · Laboratory for Computational Sensing + Robotics · BIGSS · ARCADE 116

Slide Credit: Cong Gao, *Fluoroscopic Navigation for Robot-Assisted Orthopedic Surgery*, PhD Dissertation Defense, August 2022

Copyright 2023 R. H. Taylor

Engineering Research Center for Computer Integrated Surgical Systems and Technology

119